Identifying characteristic signatures between soil moisture and heterotrophic soil respiration

by

Lasanthika Nishadini Widanagamage

B.S., University of Peradeniya, Sri Lanka, 2019
M.S., University of Peradeniya, Sri Lanka, 2022

A THESIS

submitted in partial fulfillment of the requirements for the degree

MASTER OF SCIENCE

Department of Agronomy
College of Agriculture

KANSAS STATE UNIVERSITY
Manhattan, Kansas

2024

Approved by:

Major Professor
Andres Patrignani

Copyright

Abstract

Heterotrophic soil respiration is the release of carbon dioxide (CO_2) from the soil that originates from the microbial decomposition of soil organic matter. Recognizing how this process responds to management and environmental factors is crucial for predicting changes in soil carbon levels and assessing the potential impact of climate change on terrestrial carbon stocks. This dissertation delves into the connection between heterotrophic soil respiration, soil temperature, soil moisture, and land cover using a series of laboratory and field experiments. The first chapter of this research explores the relationship between heterotrophic soil respiration and soil water potential using undisturbed soil samples collected from three different, but adjacent, land covers with the same soil textural class. The study investigates the impact of land cover in heterotrophic soil respiration and emphasizes the role of soil water potential in regulating the dynamics of this process. The second part of the study examines the link between heterotrophic soil respiration, soil temperature, and soil moisture by combining *in situ* measurements of soil CO_2 emissions with *in situ* soil water retention curves. Using asset of instrumented collars, this chapter describes an innovative alternative to measuring collocated soil matric potential, soil temperature, volumetric water content, and heterotrophic soil respiration. Our findings show the importance of conducting *in situ* measurements, particularly in well-aggregated soils, to improve the soil respiration–soil moisture relationship used by mechanistic models to better forecast terrestrial carbon stocks under different climate change scenarios.

Table of Contents

List of Figures

List of Tables

Acknowledgements

I extend my heartfelt appreciation to my parents, as well as my dear sister and brother, for their support that has illuminated my path throughout my journey. Their unwavering belief in me has been my guiding light. My deepest gratitude, however, belongs to my graduate advisor, Dr. Andres Patrignani, for entrusting me with the extraordinary opportunity to pursue my M.S. degree. His guidance and unwavering support have been the cornerstone of this achievement and for that, I am forever grateful.

I must also express my sincere gratitude to my esteemed committee members, Dr. Charles Rice and Dr. Eduardo Alvarez Santos, whose invaluable insights and feedback have been instrumental in shaping my academic pursuits.

In addition, I am profoundly grateful to my cherished friends and lab mates whose friendship and support, both in the realm of academia and in the realm of the heart, have been an enduring source of strength and inspiration.

Dedication

To my parents who always picked me up on time and encouraged me to go to every adventure and achieve every dream, specially this one!

Chapter 1 - General Introduction

Heterotrophic soil respiration (R_h) represents the soil CO_2 efflux during the decomposition of soil organic matter by soil microorganisms and it is one of the major processes of the terrestrial carbon (C) cycle (Hursh et al., 2017). Fundamental knowledge about the relationship between R_h and environmental factors controlling the R_h is crucial to improve our understanding of potential R_h rates in response to climate change. The main factors influencing R_h rate include substrate quality and availability (Hobbie et al., 2000), soil temperature (Christensen et al., 1999; Neff & Hooper, 2002), and soil moisture (Cook & Orchard, 2008; Gulledge & Schimel, 1998; Schimel et al., 1999).

The carbon chemistry of the substrate has a strong influence on the rate of microbial activity, where litter with high lignin contents and low soluble carbohydrate levels (e.g., evergreen leaf litter, woody stems) tend to decompose more slowly while substrates with low lignin contents and high soluble carbohydrate levels (i.e., deciduous and forb leaf litter) typically decompose more rapidly (Hobbie et al., 2000). In a study investigating substrate quality using community level physiological profiles (CLPPs), Priha et al. (2001) observed that litter from broadleaf forests had elevated microbial activities over litter from coniferous forests due to greater amounts of water-soluble sugars, amino acids, and organic acids. In another study investigating substrate availability conducted on forest microbial communities and their substrate utilization patterns in tropical, temperate, and boreal forests, researchers concluded that substrate availability and climatic factors dominate microbial activities and R_h rates (Fang et al., 2014).

Among all the variables affecting R_h, temperature has been the most intensively examined variable (Yuste et al., 2007), where a wide range of field (Lloyd & Taylor, 1994; Raich & Schlesinger, 1992; Rodeghiero & Cescatti, 2005) and laboratory studies (Fang & Moncrieff, 2001; Reichstein et al., 2005) have identified temperature as a key determinant of

R_h rates. This is primarily due to the strong dependence of chemical reactions and enzymatic activity to temperature. Within the typical range of field temperature conditions, the response of R_h to temperature is often described using an Arrhenius-type exponential function that eventually reaches a plateau or decreases at high temperatures (Bradford et al., 2008; Eliasson et al., 2005; Luo et al., 2001; Zhou et al., 2014). As a result, temperature sensitivity of R_h is often described as the increase in R_h with a rise of temperature by 10 °C (Q10 factor) (Luo et al., 2001). For example, R_h increases with increasing soil temperatures up to about 40 °C and further increasing soil temperature leads to constant or even a reduction of R_h rates (Hamdi et al., 2011; Knorr et al., 2005). In addition to the well-known link between temperature and enzymatic activity, modeling studies suggest that declining R_h rates at high soil temperatures may be attributed to limiting substrate availability where R_h rates start to decline as a result of a reduction in the available labile C pool due to elevated microbial activities (Hartley et al., 2007; Kirschbaum, 2004; Knorr et al., 2005). Researchers also hypothesize that the change in soil microbial community composition in response to greater temperatures caused by climate change could affect R_h at higher temperatures as the new optimal temperature shifts as microbial communities adapt to new environments (Luo et al., 2001; Zhang et al., 2005; Zogg et al., 1997). Even though the temperature sensitivity of R_h in terms of the Q10 factor has been considered constant (i.e., 2) over the past few decades, recent studies show that the Q10 factor is not constant and that other environmental factors such as soil moisture and substrate availability can affect the temperature sensitivity of R_h (Cook & Orchard, 2008; Davidson & Janssens, 2006; Luo et al., 2001).

Another important variable controlling R_h is soil moisture, which is vital for both plant growth (Huxman et al., 2004; Rodriguez-Iturbe and Porporato, 2004) and soil microbial activity. Many researchers have discussed and studied the fundamental relationship between soil moisture and R_h in the past few decades (Hui & Luo, 2004; Moyano et al., 2013; Orchard

& Cook, 1983; Raich & Schlesinger, 1992). Moisture in terms of precipitation affects biomass production and the overall input of carbon into the soil, as well as it has a direct impact on R_h and the release of carbon from the soil (Raich and Schlesinger, 1992; Parton et al., 2007). According to previous studies, intermediate soil moisture contents (i.e., 0.6 water-filled porosity) were found to be optimal for R_h where above or below soil moisture contents tend to suppress R_h (Linn & Doran, 1984; Reichstein et al., 2003). The decrease of R_h rates at high moisture contents could be attributed to limited gas diffusion through the porous matrix of very wet soils (e.g., near saturation conditions). In contrast, the restricted movement of water-soluble substrates could cause R_h rate reduction in very dry soils (Linn & Doran, 1984). Also, soil moisture has a direct impact on soil microbial population size and composition as well. For example, some microbial groups (e.g., fungi) are more resistant to drought conditions than other microbial groups (Nakas & Klein, 1979; Schnürer et al., 1986).

Except for these individual effects of soil moisture and soil temperature on R_h, the rate of R_h may vary with the combined effect of soil temperature and soil moisture (Lessard et al., 1994; Raich & Tufekciogul, 2000a; Tufekcioglu et al., 2001). Generally, high temperatures are associated with low soil moisture levels whereas high moisture levels reduce soil temperature (Davidson et al., 1998). This strong interdependency makes separating individual effects of soil moisture and temperature difficult and the transferability of inferences made by laboratory studies considering temperature or soil moisture to real-world scenarios questionable (Bauer et al., 2012).

Recent research suggests that global warming may stimulate R_h rates in wet areas, where most of the world's soil organic carbon storages are concentrated, which could increase net CO_2 emissions in the near future (Zhou et al., 2014). According to Cox et al. (2000), the positive response of R_h to rising temperatures may enhance the loss of soil carbon from terrestrial ecosystems and act as a positive feedback to climate change. The

Intergovernmental Panel on Climate Change (IPCC) (2013) has predicted a rise in average temperatures and a heightened occurrence of extreme events, including droughts, floods, and heat waves, as a result of climate change, which would mostly likely affect R_h dynamics. Satellite data of 35 years from 1982 shows that global tree cover has increased by 7.1% compared to the 1982 level and bare ground cover has decreased by 3.1% specifically in agricultural regions (Song et al., 2018). Given recent forecasts of global climate change and land cover changes, accurate knowledge of the response of R_h to soil moisture and temperature will be critical for accurate predictions of soil carbon storage changes (Davidson & Janssens, 2006). Therefore, this thesis is focused on further investigating the relationship between soil moisture and R_h in three different land covers under laboratory conditions using undisturbed soil samples and studying the response of R_h to soil moisture and temperature dynamics under field conditions in a tallgrass prairie in central Kansas.

.

References

Bauer, J., Weihermüller, L., Huisman, J. A., Herbst, M., Graf, A., Séquaris, J. M., & Vereecken, H. (2012). Inverse determination of heterotrophic soil respiration response to temperature and water content under field conditions. *Biogeochemistry*, *108*(1–3), 119–134. https://doi.org/10.1007/s10533-011-9583-1

Bradford, M. A., Davies, C. A., Frey, S. D., Maddox, T. R., Melillo, J. M., Mohan, J. E., Reynolds, J. F., Treseder, K. K., & Wallenstein, M. D. (2008). Thermal adaptation of soil microbial respiration to elevated temperature. *Ecology Letters*, *11*(12), 1316–1327. https://doi.org/10.1111/j.1461-0248.2008.01251.x

Christensen, T. R., Jonasson, S., Callaghan, T. V., & Havström, M. (1999). On the potential CO_2 release from tundra soils in a changing climate. *Applied Soil Ecology*, *11*(2–3), 127–134. https://doi.org/10.1016/S0929-1393(98)00146-2

Cook, F. J., & Orchard, V. A. (2008). Relationships between soil respiration and soil moisture. *Soil Biology and Biochemistry*, *40*(5), 1013–1018. https://doi.org/10.1016/j.soilbio.2007.12.012

Cox, P. M., Betts, R. A., Jones, C. D., Spall, S. A., & Totterdell, I. J. (2000). Acceleration of global warming due to carbon-cycle feedbacks in a coupled climate model. *Nature*, *408*(6809), 184–187. https://doi.org/10.1038/35041539

Curiel Yuste, J., Baldocchi, D. D., Gershenson, A., Goldstein, A., Misson, L., & Wong, S. (2007). Microbial soil respiration and its dependency on carbon inputs, soil temperature, and moisture. *Global Change Biology*, *13*(9), 2018–2035. https://doi.org/10.1111/j.1365-2486.2007.01415.x

Davidson, E. A., & Janssens, I. A. (2006). Temperature sensitivity of soil carbon decomposition and feedbacks to climate change. *Nature*, *440*(7081), 165–173. https://doi.org/10.1038/nature04514

Davidson, Eric. A., Belk, E., & Boone, R. D. (1998). Soil water content and temperature as independent or confounded factors controlling soil respiration in a temperate mixed hardwood forest. *Global Change Biology*, *4*(2), 217–227. https://doi.org/10.1046/j.1365-2486.1998.00128.x

Eliasson, P. E., McMurtrie, R. E., Pepper, D. A., Strömgren, M., Linder, S., & Ågren, G. I. (2005). The response of heterotrophic CO_2 flux to soil warming. *Global Change Biology*, *11*(1), 167–181. https://doi.org/10.1111/j.1365-2486.2004.00878.x

Fang, C., & Moncrieff, J. B. (2001). The dependence of soil CO_2 efflux on temperature. *Soil Biology and Biochemistry*, *33*(2), 155–165. https://doi.org/10.1016/S0038-0717(00)00125-5

Fang, H., Cheng, S., Wang, Y., Yu, G., Xu, M., Dang, X., Li, L., & Wang, L. (2014). Changes in soil heterotrophic respiration, carbon availability, and microbial function in seven forests along a climate gradient. *Ecological Research*, *29*(6), 1077–1086. https://doi.org/10.1007/s11284-014-1194-6

Gulledge, J., & Schimel, J. P. (1998). Moisture control over atmospheric CH_4 consumption and CO_2 production in diverse Alaskan soils. *Soil Biology and Biochemistry*, *30*(8–9), 1127–1132. https://doi.org/10.1016/S0038-0717(97)00209-5

Hamdi, S., Chevallier, T., Ben Aïssa, N., Ben Hammouda, M., Gallali, T., Chotte, J.-L., & Bernoux, M. (2011). Short-term temperature dependence of heterotrophic soil respiration after one-month of pre-incubation at different temperatures. *Soil Biology and Biochemistry*, *43*(9), 1752–1758. https://doi.org/10.1016/j.soilbio.2010.05.025

Hartley, I. P., Heinemeyer, A., & Ineson, P. (2007). Effects of three years of soil warming and shading on the rate of soil respiration: Substrate availability and not thermal acclimation mediates observed response. *Global Change Biology*, *13*(8), 1761–1770. https://doi.org/10.1111/j.1365-2486.2007.01373.x

Hobbie, S. E., Schimel, J. P., Trumbore, S. E., & Randerson, J. R. (2000). Controls over carbon storage and turnover in high-latitude soils. *Global Change Biology*, *6*(S1), 196–210. https://doi.org/10.1046/j.1365-2486.2000.06021.x

Hui, D., & Luo, Y. (2004). Evaluation of soil CO_2 production and transport in Duke Forest using a process-based modeling approach. *Global Biogeochemical Cycles*, *18*(4), 2004GB002297. https://doi.org/10.1029/2004GB002297

Hursh, A., Ballantyne, A., Cooper, L., Maneta, M., Kimball, J., & Watts, J. (2017). The sensitivity of soil respiration to soil temperature, moisture, and carbon supply at the global scale. *Global Change Biology*, *23*(5), 2090–2103. https://doi.org/10.1111/gcb.13489

Kirschbaum, M. U. F. (2004). Soil respiration under prolonged soil warming: Are rate reductions caused by acclimation or substrate loss? *Global Change Biology*, *10*(11), 1870–1877. https://doi.org/10.1111/j.1365-2486.2004.00852.x

Knorr, W., Prentice, I. C., House, J. I., & Holland, E. A. (2005). Long-term sensitivity of soil carbon turnover to warming. *Nature*, *433*(7023), 298–301. https://doi.org/10.1038/nature03226

Lessard, R., Rochette, P., Topp, E., Pattey, E., Desjardins, R. L., & Beaumont, G. (1994). Methane and carbon dioxide fluxes from poorly drained adjacent cultivated and forest sites. *Canadian Journal of Soil Science*, *74*(2), 139–146. https://doi.org/10.4141/cjss94-021

Linn, D. M., & Doran, J. W. (1984). Effect of water-filled pore space on carbon dioxide and nitrous oxide production in tilled and non-tilled soils. *Soil Science Society of America Journal*, *48*(6), 1267–1272. https://doi.org/10.2136/sssaj1984.03615995004800060013x

Lloyd, J., & Taylor, J. A. (1994). On the temperature dependence of soil respiration. *Functional Ecology*, *8*(3), 315. https://doi.org/10.2307/2389824

Luo, Y., Wan, S., Hui, D., & Wallace, L. L. (2001). Acclimatization of soil respiration to warming in a tall grass prairie. *Nature*, *413*(6856), 622–625. https://doi.org/10.1038/35098065

Moyano, F. E., Manzoni, S., & Chenu, C. (2013). Responses of soil heterotrophic respiration to moisture availability: An exploration of processes and models. *Soil Biology and Biochemistry*, *59*, 72–85. https://doi.org/10.1016/j.soilbio.2013.01.002

Nakas, J. P., & Klein, D. A. (1979). Decomposition of microbial cell components in a semi-arid grassland soil. *Applied and Environmental Microbiology*, *38*(3), 454–460. https://doi.org/10.1128/aem.38.3.454-460.1979

Neff, J. C., & Hooper, D. U. (2002). Vegetation and climate controls on potential CO_2, DOC and DON production in northern latitude soils: Climate and vegetation controls over soil organic matter dynamics. *Global Change Biology*, *8*(9), 872–884. https://doi.org/10.1046/j.1365-2486.2002.00517.x

Orchard, V. A., & Cook, F. J. (1983). Relationship between soil respiration and soil moisture. *Soil Biology and Biochemistry*, *15*(4), 447–453. https://doi.org/10.1016/0038-0717(83)90010-X

Priha, O., Grayston, S. J., Hiukka, R., Pennanen, T., & Smolander, A. (2001). Microbial community structure and characteristics of the organic matter in soils under *Pinus sylvestris*, *Picea abies* and *Betula pendula* at two forest sites. *Biology and Fertility of Soils*, *33*(1), 17–24. https://doi.org/10.1007/s003740000281

Raich, J. W., & Schlesinger, W. H. (1992). The global carbon dioxide flux in soil respiration and its relationship to vegetation and climate. *Tellus B*, *44*(2), 81–99. https://doi.org/10.1034/j.1600-0889.1992.t01-1-00001.x

Raich, J. W., & Tufekciogul, A. (2000). Vegetation and soil respiration: Correlations and controls. *Biogeochemistry*, *48*(1), 71–90. https://doi.org/10.1023/A:1006112000616

Reichstein, M., Rey, A., Freibauer, A., Tenhunen, J., Valentini, R., Banza, J., Casals, P., Cheng, Y., Grünzweig, J. M., Irvine, J., Joffre, R., Law, B. E., Loustau, D., Miglietta, F., Oechel, W., Ourcival, J., Pereira, J. S., Peressotti, A., Ponti, F., … Yakir, D. (2003). Modeling temporal and large-scale spatial variability of soil respiration from soil water availability, temperature and vegetation productivity indices. *Global Biogeochemical Cycles*, *17*(4), 2003GB002035. https://doi.org/10.1029/2003GB002035

Reichstein, M., Subke, J., Angeli, A. C., & Tenhunen, J. D. (2005). Does the temperature sensitivity of decomposition of soil organic matter depend upon water content, soil horizon, or incubation time? *Global Change Biology*, *11*(10), 1754–1767. https://doi.org/10.1111/j.1365-2486.2005.001010.x

Rodeghiero, M., & Cescatti, A. (2005). Main determinants of forest soil respiration along an elevation/temperature gradient in the Italian Alps. *Global Change Biology*, *11*(7), 1024–1041. https://doi.org/10.1111/j.1365-2486.2005.00963.x

Schimel, J. P., Gulledge, J. M., Clein-Curley, J. S., Lindstrom, J. E., & Braddock, J. F. (1999). Moisture effects on microbial activity and community structure in decomposing birch litter in the Alaskan taiga. *Soil Biology and Biochemistry*, *31*(6), 831–838. https://doi.org/10.1016/S0038-0717(98)00182-5

Schnürer, J., Clarholm, M., Boström, S., & Rosswall, T. (1986). Effects of moisture on soil microorganisms and nematodes: A field experiment. *Microbial Ecology*, *12*(2), 217–230. https://doi.org/10.1007/BF02011206

Song, X. P., Hansen, M. C., Stehman, S. V., Potapov, P. V., Tyukavina, A., Vermote, E. F., & Townshend, J. R. (2018). Global land change from 1982 to 2016. *Nature*, *560*(7720), 639-643.

Stocker, T. (Ed.). (2014). *Climate change 2013: The physical science basis: Working Group I contribution to the Fifth assessment report of the Intergovernmental Panel on Climate Change*. Cambridge University Press.

Tufekcioglu, A., Raich, J. W., Isenhart, T. M., & Schultz, R. C. (2001). Soil respiration within riparian buffers and adjacent crop fields. *Plant and Soil*, *229*(1), 117–124. https://doi.org/10.1023/A:1004818422908

Zhang, W., Parker, K. M., Luo, Y., Wan, S., Wallace, L. L., & Hu, S. (2005). Soil microbial responses to experimental warming and clipping in a tallgrass prairie. *Global Change Biology*, *11*(2), 266–277. https://doi.org/10.1111/j.1365-2486.2005.00902.x

Zhou, W., Hui, D., & Shen, W. (2014). Effects of soil moisture on the temperature sensitivity of soil heterotrophic respiration: A laboratory incubation study. *PLoS ONE*, *9*(3), e92531. https://doi.org/10.1371/journal.pone.0092531

Zogg, G. P., Zak, D. R., Ringelberg, D. B., White, D. C., MacDonald, N. W., & Pregitzer, K. S. (1997). Compositional and functional shifts in microbial communities due to soil warming. *Soil Science Society of America Journal*, *61*(2), 475–481. https://doi.org/10.2136/sssaj1997.03615995006100020015x

Chapter 2 - Study of Heterotrophic Soil Respiration as a Function of Soil Water Potential under Different Land Covers

Nishadini Widanagamage, Charles Rice, Eduardo Santos, and Andres Patrignani

Abstract

Soil organic carbon (SOC) is a critical component of the terrestrial carbon cycle, with heterotrophic soil respiration (R_h) representing a major pathway through which carbon is released into the atmosphere. The objective was to investigate the relationship between R_h and soil water potential (Ψ_w) using undisturbed soil samples from different land covers, including croplands, grasslands, and riparian areas in central Kansas. Soil CO_2 efflux and soil matric potential were simultaneously measured in 5 cm depth undisturbed soil samples (250 cm^3) under laboratory conditions (22 ± 1 ^oC) by combining mini precision tensiometers (model Hyprop 2, Meter Group, Inc.) and a CO_2 gas analyzer (model EGM-5, PP Systems, Inc.). Soil pH, EC, CEC, organic matter%, total N% and total C% were analyzed as soil chemical properties while PLFA was conducted to identify soil microbial composition. The results reveal that mean R_h rates in different land covers were significantly different (P<0.001) where croplands showed R_h = 0.40 (SD = 0.08) µmol m^{-2} s^{-1} compared to riparian R_h = 0.81 (SD = 0.24) µmol m^{-2} s^{-1} and grassland areas R_h = 0.92 (SD = 0.10) µmol m^{-2} s^{-1}. The study demonstrates that soil moisture substantially impacts R_h, with peak R_h occurring within the proximity of field capacity (i.e. -10 kPa) regardless of the land cover. Interestingly, results illustrate that maximum R_h occurs ~0.8 water-filled porosity in all three studied land covers. Using undisturbed soil samples along with the coupling of mini-precision tensiometers and a respiration chamber provided valuable insights into the R_h –Ψ_w relationship under laboratory conditions that could be implemented in future studies aiming at better understanding soil carbon dynamics in the face of climate change.

Introduction

Soil organic carbon (SOC) is the largest reservoir of terrestrial carbon (C), which results from the balance of C inputs (e.g., leaf and root debris) and outputs (e.g., CO_2, CH_4 emissions) in the soil. This reservoir of SOC can be released back into the atmosphere by soil respiration (R_s), which consists of autotrophic respiration (R_a, from plants) and heterotrophic respiration (R_h, involving soil microbes and fauna), and constitutes one of the major fluxes in the terrestrial C cycle totaling 98 ± 12 Pg C yr^{-1} (Bond-Lamberty & Thomson, 2010). As a result of its vital role in the global C cycle and its possible feedback on climate change, accurate predictions of soil CO_2 efflux in response to shifting environmental conditions are essential to forecast terrestrial carbon stocks. The rates of R_h are mainly influenced by key factors like soil moisture (Gulledge & Schimel, 1998; Schimel et al., 1999), soil temperature (Christensen et al., 1999; Neff & Hooper, 2002), and substrate quality and availability (Hobbie et al., 2000). While numerous studies in the scientific literature have extensively examined the response of R_h to soil temperature (Bond-Lamberty & Thomson, 2010; Bradford et al., 2008; Zhang et al., 2005), there remains a gap in our understanding of the response of R_h to changes soil moisture conditions in terms of soil water potential (Novick et al., 2022).

Understanding the response of R_h to soil moisture is critical for better understanding biogeochemical processes and reducing conceptual and modeling uncertainties for predicting the fate of SOC stocks, global greenhouse gas emissions, and future atmospheric composition in the face of climate change (Johnson et al., 2013; Moyano et al., 2013). Despite the consensus in modeling analyses and climate change studies regarding the substantial influence of R_h on global warming, the available evidence on its sensitivity to changes in soil moisture conditions is limited (Carey et al., 2016; Schindlbacher et al., 2009; Wang et al., 2014). Earth system models typically rely on physically-based relationships between soil

moisture and soil carbon transformations, but current soil moisture– R_h relationships remain primarily defined as simple empirical functions which could lead to large uncertainties in the predictions and projections of R_h rates (Hawkes et al., 2017; Novick et al., 2022). Thus, a more physically sound function to describe the relationship between soil moisture and R_h has the potential to reduce uncertainties in R_h predictions across soils with a wide range of textures and structures (Ghezzehei et al., 2019; Yan et al., 2018).

Soil moisture dynamics affect R_h by controlling the production and diffusion of CO_2 within the soil porous matrix. As the soil matric potential decreases (i.e., becomes more negative), films of pore water become more tightly bound to the surfaces of soil aggregates, leading to reduced water availability (Ilstedt et al., 2000a). This, in turn, results in a limitation of substrate and nutrient diffusion, which can subsequently lead to microbial substrate scarcity and physiological stress (Stark & Firestone, 1995). For instance, high soil moisture contents can reduce gas diffusion rates and suppress O_2 supply to microbes. In contrast, low soil moisture conditions can inhibit the diffusion and advection of solutes within the pore solution, and limit nutrients and substrate availability for microbes thus suppressing microbial activity and lowering R_h rates (Manzoni et al., 2012). In the long-term, soil water deficits affect the primary production of ecosystems, thus reducing the input of organic carbon back into the soil and lowering substrate abundance for microbial decomposition and R_h (Goetz et al., 2005).

Most previous studies that investigated the relationship between R_h and soil moisture conditions have used gravimetric and volumetric soil moisture indicators (Wickland & Neff, 2008; Yan et al., 2018), which are typically simpler to determine in laboratory and field conditions compared to measuring soil water potential. This approach could potentially hinder a more fundamental understanding of the relationship between soil moisture and R_h across soils with different particle and pore size distributions. Only a few studies have used

soil water potential as a soil moisture indicator, but to our knowledge, previous studies have mostly relied on disturbed soil samples to measure R_h at a few selected Ψ_w values (Conant et al., 2004; Fischer, 2009; Orchard & Cook, 1983; Yan et al., 2016). In some previous studies, researchers suggest that drying and sieving practices related to soil processing and conditioning in soil respiration studies could alter microbial community composition, microbial biomass, and substrate availability, questioning the applicability of results in real-world conditions (Herbst et al., 2016). Therefore, there is a need to investigate further the Ψ_w– R_h relationship using undisturbed soil samples to improve the understanding of R_h as a function of the energy state of the soil moisture (i.e., soil water potential). We hypothesize that soils under contrasting land uses exhibit distinct signatures of the Ψ_w– R_h relationship, enabling a more accurate representation of soil respiration as a function of transient soil moisture conditions than using gravimetric or volumetric soil moisture indicators. The objective of this study was to identify the signatures of the relationship between R_h and Ψ_w under transient soil moisture conditions using undisturbed soil samples obtained from different, but adjacent, land covers.

Materials and Methods

Site selection and soil sampling

For this study, we selected a total of nine sites across central Kansas with adjacent land cover types representing one of the following vegetation pairs: cropland-grassland, cropland-riparian, or grassland-riparian (Table 2-1). Site selection criteria was based on two conditions: 1) consistent land cover over the past 30 years, verified through historical satellite image analysis, and 2) matching soil series for both land cover types based on the Natural Resources Conservation Service (NRCS) Web Soil Survey Geodatabase (Figure 2-1). Both conditions were enforced to ensure that differences in soil respiration responses to changes in

soil matric potential were mostly attributed to land cover effects and associated microbial populations. Cropland fields were characterized by typical crop rotations of the region, which included corn (*Zea mays*), soybeans (*Glycine max*), and winter wheat (*Triticum aestivum*). All grassland sites were located within the Konza Prairie Biological Station and were composed by tall grasses like big bluestem (*Andropogan gerardi*) and switchgrass (*Panicum virgatum*) and short grasses like little bluestem (*Schizachyrium scoparium*) and Indiangrass (*Sorghastrum nutans*). Riparian areas were mostly dominated by Black Walnut (*Juglans nigra*), Bur Oak (*Quercus macrocarpa*), Eastern Cottonwood (*Populus deltoides*), Honey Locust (*Gleditsia triacanthos*), and Sycamore (*Platanus occidentalis*) tree species.

Undisturbed soil cores with a volume of 250 cm^3 (8 cm inner diameter and 5 cm in height) were collected in triplicate in the 0 to 5 cm soil layer in each land cover at the nine selected sites. Any layer of plant residue and partially decomposed litter was removed to ensure samples were obtained in the layer of mineral soil. Undisturbed soil cores were used in the laboratory to simultaneously measure soil matric potential, volumetric water content, and soil CO_2 efflux. In addition, at each land cover site, we collected a composite soil sample in the top 5 cm that was split into three subsamples for phospholipid fatty acid (PLFA) analysis, soil chemical analysis, and particle size analysis. All soil samples were stored in an insulated box during field sampling. Soil samples for PLFA analysis were frozen at -18 °C overnight and then sent to a commercial laboratory (Ward Laboratories, Kearney, NE). All other soil samples were stored at 4 °C for a maximum of six weeks following the recommendations of previous research studies (Meyer et al., 2019). Soil chemical analyses included cation exchange capacity by the ammonium-ion replacement method, organic matter content by the loss on ignition method, total nitrogen and total carbon on a weight percent basis, and pH and bulk electrical conductivity (EC_b) by saturated paste method (1:1 soil:deionized water) using a calibrated pH and conductivity meter (model PC100, Cole-Parmer, Inc.). Particle size

analysis was determined using the hydrometer method (Gavlak et al., 2005). Since some soils had high (i.e., >3.5%) organic matter content, all samples were treated with laboratory-grade 30% hydrogen peroxide solution before particle size analysis (Gavlak et al., 2005). Soil sampling was concentrated between March and July 2023 and no more than three sites were sampled at the same time to ensure that soil samples were storage for less than six weeks.

Soil matric potential and water-filled porosity measurements

The bottom side of the undisturbed soil cores was covered with a cheesecloth secured with a rubber band and saturated from the bottom up in a 5 mM $CaCl_2$ solution. The saturated samples were weighed without the cheesecloth to determine the effective saturation of the soil. Then, the saturated soil samples were immediately mounted on the Hyprop system (model Hyprop 2, Meter Group, Inc.), which is an automated hydraulic property analyzer that consists of two precision mini-tensiometers that are 3.0 cm and 5.0 cm long and that measure the wet-end (i.e., 0 to -80 kPa) of the soil water retention curve based on the Wind-Schindler's evaporation method (Schindler & Müller, 2006). Throughout the run, soil matric potential (Ψ_m) was continuously recorded by the associated Hyprop software. The mass of each Hyprop sensor head with the mounted undisturbed soil core was recorded between two and four times per day as recommended by the manufacturer's manual. For each timestamp, the average matric potential of each soil sample was computed as the average of both precision mini-tensiometers. Hyprop readings were terminated when the tensiometers cavitated at around -80 kPa or when soil respiration was negligible. After dismounting the soil from the Hyprop system, soil water potential was determined in four to six subsamples from each soil core using a dew point soil water potential meter (model WP4C, Meter Group, Inc.) which uses the chilled mirror dew point technique to measure water potentials in the range from 0.1 to 300 MPa, which allowed us to extend measurements of soil water potential

beyond the tensiometer range. Volumetric soil water contents for each Hyprop sample and the subsamples analyzed with the dew point water potential meter were determined using the thermo-gravimetric method. The osmotic potential (Ψ_o, kPa) of each sample was estimated as a function of the sample volumetric water content (θ, $cm^3\ cm^{-3}$) and the EC_b ($dS\ m^{-1}$) of the saturation paste extract (Andraski & Scanlon, 2018):

$$\Psi_o = -36\ EC_b\ \frac{\theta_s}{\theta} \qquad \text{[Eq. 2-1]}$$

where, θ_s ($cm^3\ cm^{-3}$) is the saturated volumetric water content. To describe the soil water retention curve, we fitted the van Genuchten model (Eq. 2-2) (van Genuchten, 1980):

$$\frac{\theta - \theta_r}{\theta_s - \theta_r} = [1 + (-\alpha\ \psi_m)^n]^{-m} \qquad \text{[Eq. 2-2]}$$

where, θ_r ($cm^3\ cm^{-3}$) is residual volumetric water content, Ψ_m (kPa) is soil matric potential, and $\alpha, n,$ and m are fitting parameters where $m = 1 - 1/n$. In this study we assumed that field capacity is the volumetric water content held at -10 kPa matric potential.

Water-filled porosity (WFP) represents the fraction of the pore space filled with water and is another common metric to describe soil moisture conditions within the context of soil respiration (Ilstedt et al., 2000; Torbert & Wood, 1992). In this study, we computed WFP (unitless) as follows:

$$WFP = \frac{\theta}{f} \qquad \text{[Eq. 2-3]}$$

where f (unitless) is the total porosity of the soil estimated as $f = \rho_b/\rho_s$, ρ_b ($g\ cm^{-3}$) is the bulk density of the soil obtained after oven drying the undisturbed soil cores at 105 ºC for 48 hours, and ρ_s ($g\ cm^{-3}$) is the particle density of the mineral fraction, which was assumed to be approximately 2.65 $g\ cm^{-3}$ based on a previous study that measured ρ_s for soils in this region (Parker et al., 2022).

Soil CO_2 efflux measurements

Soil CO_2 efflux was measured simultaneously during measurements of soil matric potential with a handheld infrared CO_2 gas analyzer (model EGM-5, PP Systems, Inc.) under laboratory conditions (21 ± 1 °C). Soil CO_2 efflux was measured multiple times per day from saturation conditions until both tensiometers cavitated and until soil CO_2 efflux readings became negligible, with an approximate difference in CO_2 concentration (dC) between two consecutive readings approaching zero. Each measurement of soil CO_2 efflux spanned 180 seconds. A custom 3D-printed polylactic acid (PLA) plastic collar was used to couple the chamber of the handheld infrared CO_2 gas analyzer with the samples of the Hyprop system. Soil CO_2 efflux was not measured in the dry end of the soil water retention curve measured with the water potential meter since this technique requires the use of small and disturbed soil samples and soil CO_2 efflux readings were usually negligible near cavitation of the tensiometers of the Hyprop system. Soil CO_2 efflux was computed as follows:

$$F_{CO2} = \frac{dC}{dt}\ \frac{P}{1013}\ \frac{273}{273+T_{air}}\ \frac{1}{22.414}\ \frac{V}{A}\ 10^3 \qquad \text{[Eq. 2-4]}$$

where F_{CO2} (µmol m^{-2} s^{-1}) is the soil CO_2 efflux, dC (ppm) is the change in CO_2 concentration, dt (s) is the change in measurement time, $\frac{P}{1013}$ is the correction for barometric pressure with P (mbar) measured by the EGM-5, $\frac{1}{22.414}$ (mol m^{-3}) is the standard molar volume of an ideal gas, $\frac{273}{273+T_{air}}$ is the correction for air temperature with T_{air} (°C) input by the user, V (m^3) is the chamber volume, and A (m^2) is the soil surface area, which in this case was the area of 4.9×10^{-3} m^2 of the stainless steel rings holding the undisturbed soil samples. The rate of change in CO_2 concentration (i.e., dC/dt) was estimated using linear regression analysis based on the data collected between the 30- and 150-seconds mark.

Statistical analysis

To analyze the statistical significance of soil physical, chemical, and biological properties between each pair of two adjacent land covers student's T-test and among the three land cover pairs one-way ANOVA was used at the 5% significance level. Linear regression analysis and the Pearson correlation coefficient were used to investigate the Ψ_w– R_h relationship. Curve fitting of the van Genuchten soil water retention model was implemented using the *curve fit* function within the SciPy module in the Python programming language.

Results and Discussion

Relationship of soil CO_2 efflux with soil matric potential and water-filled porosity

As expected, R_h approached a low value at both near-saturation conditions (WFP = 1, Ψ_m = 0 kPa) and low soil moisture contents (WFP < 0.2, Ψ_m < -1,000 kPa). At high soil moisture contents, R_h is mostly restricted by pores filled with water, blocking the diffusion path of CO_2 and small respiration rates could be attributed to anaerobic respiration. An additional factor potentially contributing to the observation of R_h rates values closer to zero is the resolution of the infrared gas analyzer, especially when operating at extremely low CO2 concentrations. At low soil moisture contents, R_h is typically restricted by low water availability impairing basic physiological processes of the microbes. Because at high and low soil moisture levels R_h tends to approach zero, another important aspect towards describing the relationship between R_h and soil moisture is the Ψ_w or WFP point at which R_h is highest. The average peak R_h observed across all undisturbed soil samples collected in cropland was 0.966 (SD = 0.35) µmol m^{-2} s^{-1}, in riparian area was 1.634 (SD = 0.66) µmol m^{-2} s^{-1}, and in grasslands was 1.883 (SD = 0.16) µmol m^{-2} s^{-1}. Maximum R_h values were highest in grassland sites and was statistically different (P<0.001) among the three land covers, indicating that the

land cover likely affected the associated microbial population of the soil and the highest rate of microbial activity. Further inspection of the PLFA analysis (Table 2-2) revealed that the total microbial biomass was also highest in grassland sites, with an average of 6,275 ng g^{-1}, and lowest in cropland sites, with an average of 2,745 ng g^{-1}. The riparian sites had a mean total microbial biomass of 5,327 ng g^{-1}, which was slightly lower than the mean total microbial biomass of the grassland sites. Interestingly, the cropland:grassland and riparian:grassland ratios of maximum R_h were 0.51 and 0.87, which are somewhat similar to the cropland:grassland and riparian:grassland ratios of total microbial biomass, with values of 0.72 and 0.83, respectively.

The WFP at which the maximum R_h occurred was not statistically significant among land covers, which means that peak R_h occurred at predictable soil moisture values regardless of the land cover and soil type. The mean WFP and R_h measurements spanned the range between 0.2 and 1.0 (Figures 2-2, 2-3, and 2-4). Observations of WFP <0.2 were limited by the range of the wet end of the soil water retention curve and also due to negligible respiration rates at very low soil moisture values. Across all three land covers, the peak R_h was consistently observed at an average WFP of 0.8 (Figure 2-5). The pattern observed in the scatter plot between R_h and WFP aligns well with the response suggested by Linn & Doran (1984), but on average, the maximum soil CO_2 efflux in our study was observed at ~0.8 WFP in all three land covers, while Linn & Doran (1984) reported maximum relative microbial activity at about 0.6 WFP. A possible reason for the discrepancy between our study and previous incubation studies, including the study by Linn & Doran (1984), may be attributed to the use of disturbed soil samples that 1) alter the soil structure by breaking down aggregates and the pore network, and 2) possibly altering the microbial community composition. In terms of mean Ψ_m, the maximum R_h in cropland soil samples was observed at -13.3 kPa, in grassland samples at -6.4 kPa, and in samples from riparian areas at -4.3 kPa,

showing that maximum R_h consistently occurs in the proximity of field capacity (Figure 2-5). Furthermore, the consistency of observations in both Ψ_m and WFP values associated with maximum R_h across land covers implies that both Ψ_m and WFP serve as equally effective variables for characterizing R_h dynamics, albeit the patterns observed using WFP were more uniform and less scattered than the observed patterns using Ψ_m. Consequently, researchers may select either of these indicators depending on the availability of research resources, without a substantial compromise in the reliability of their findings. Also, the WFP at which R_h reached the maximum may be a useful indicator of relative potential for aerobic and anaerobic microbial activity in soil, with WFP <0.8 constituting a water-limiting region and WFP >0.8 representing an aeration-limiting region where R_h starts to gradually transition into anaerobic conditions. With WFP >0.8, the amount of O_2 in soil pores for microbial activities decreases as air diffusion passages are blocked by pores with increasing soil water content, which also decreases the efflux of CO_2 observed with gas chambers.

The mean osmotic potential (Ψ_o) under saturated conditions in cropland soil samples was -8.1 kPa (SD = 6.3 kPa), in riparian samples was -10.3 kPa (SD = 9.7 kPa), and in grassland samples was -5.8 kPa (SD = 3.3 kPa). In dry soils, solute concentration in the soil solution increases, dramatically decreasing Ψ_o, which can affect the activity of microbial populations. Maximum Ψ_o observed in cropland samples was only 4% of maximum Ψ_m whereas the maximum Ψ_o observed in grasslands and riparian samples was only 3% of the maximum Ψ_m. Thus, Ψ_o was not a major factor influencing soil water potential for the soil samples in this study. A laboratory experiment conducted to study the response of microbial activity to decreasing Ψ_o and Ψ_m in two non-saline soils revealed that both low Ψ_m and low Ψ_o have negative impacts on soil microbial activity and soil respiration, but low Ψ_m had a stronger impact than Ψ_o (Chowdhury et al., 2011). In other studies conducted on the effect of osmotic potential on soil CO_2 evolution, researchers have found that in the -30 to -3000 kPa

range, osmotic potential causes a non-linear reduction of soil CO_2 efflux (Johnson & Guenzi, 1963; Singh et al., 1969).

The soil samples from adjacent landcovers showed different magnitudes of mean R_h, indicating the land cover effects on R_h (Figures 2-6, 2-7, and 2-8). Mean R_h rates in samples from different land covers were significantly different, where samples from cropland had R_h = 0.40 (SD = 0.08) µmol m^{-2} s^{-1}, samples from riparian areas had R_h = 0.81 (SD = 0.24) µmol m^{-2} s^{-1}, and samples from grassland areas had R_h = 0.92 (SD = 0.10) µmol m^{-2} s^{-1}. Similarly, a study conducted in riparian buffers and adjacent cropland fields in central Iowa, USA showed that soil respiration was significantly higher in riparian buffers than adjacent croplands indicating greater biological activity in riparian buffer soils which agrees with the observations of our present study (Tufekcioglu et al., 2001). Also, another study conducted to find the correlation and controls between vegetation type and soil respiration found that coniferous forests had 10 % lower respiration rates than adjacent broadleaf forests growing on the same soil type, and grassland had 20% higher respiration rates than forest stands (Raich & Tufekciogul, 2000b). Furthermore, other studies in the scientific literature show that the soil respiration rate is lower in cultivated than adjacent forest areas (Lessard et al., 1994), and lower in harvested forests than in undisturbed forests (Striegl & Wickland, 1998).

In addition to soil temperature and soil moisture conditions, the magnitude of the soil CO_2 efflux varies depending on the microbial community composition and total microbial population size. A study conducted in a dry deciduous forest and a temperate forest in Uttar Pradesh State, India found that the forest type and tree species affect soil respiration and microbial activity (Chandra et al., 2016). Also, the standing vegetation affects the microbial community composition and activity rates. Litter quantity and quality, root extrudates vary depending on vegetation which determines the soil microclimate of microbes. Therefore, even though some soils have higher organic matter contents (Table 2-3), microbial activities

and R_h could be lower depending on other microclimate conditions of the soil. A study conducted in a secondary forest and a pine plantation in the Luquillo Experimental Forest in Puerto Rico found that different microbial groups were more responsible for R_h in different land covers (e.g. fungi in pine plantation and bacteria in secondary forest) whereas soil moisture was a major factor determining R_h in those land covers where the temperature was stable (Li et al., 2006).

Soil water retention curves

As expected, differences in soil water retention curves were mostly evident at the wet end of the curve, where soil structure plays a more dominant role, while differences at the dry end of the curve were minimal due to similar soil textural classes between adjacent land covers (Figure 2-9). On average, soil samples from riparian areas exhibited a 0.60 (SD = 0.05) cm^3 cm^{-3} mean θ_s with respect to 0.56 (SD = 0.06) cm^3 cm^{-3} in grasslands and 0.48 (SD = 0.03) cm^3 cm^{-3} mean θ_s in the studied croplands which could be attributed to a higher organic matter content (Table 2-3) and dense root systems in riparian areas. Mean organic matter content of 3.9 (SD = 1.9)% was observed in cropland soils and was 5.7 (SD = 1.6)% in grasslands 6.4 (SD = 2.8)% in riparian soils. The mean θ_s values were significantly different in cropland-riparian (P<0.05) and cropland-grassland (P <0.05) combinations, but the difference was not statistically significant in grassland-riparian (P = 0.52) pairs. The largest discrepancy in saturation within a site was observed in site 1, where a cropland-riparian combination showing a greater effect of land cover and management practices on soil physical properties (Table 2-4 and Table 2-5). Regardless of the soil type, all cropland soil samples exhibited a lower θ_s with respect to soil samples collected in adjacent riparian or grassland areas with having an average 0.11 cm^3 cm^{-3} difference in cropland:riparian combination and 0.05 cm^3 cm^{-3} average difference in cropland:grassland combination. The

likely effect of frequent farming operations and continuous cropping on the mineralization of soil organic matter and the associated loss of soil structure and aggregate stability could have led to this lower θ_s in cropland soils.

Variation of soil chemical and physical properties across sites and land covers

Soil chemical and physical properties are often used to assess the soil quality of an ecosystem (Kekane, 2015). The main soil chemical properties analyzed in this study included soil pH, organic matter content, and C:N ratio which are critical factors influencing soil microbial activity with far-reaching consequences for soil health, nutrient cycling, and ecosystem sustainability. Among the studied sites, soil pH ranged from 5.0 to 7.2 in croplands, from 6.2 to 7.3 in grasslands, and from 6.2 to 7.5 in riparian areas, indicating that riparian and grasslands soils had neutral pH whereas cropland soils were slightly more acidic (Table 2-3). Only pH values in the cropland-riparian combination were significantly different (P<0.05) between land covers. Soil microbial activity typically thrives with pH values ranging from 6 to 7.5, thus, the lower pH values observed in cropland sites could have been partially responsible for to reduced R_h. All the studied sites had organic matter contents >3%, except for the cropland field at site 2, which had a value of 1.3% (Table 2-3). Interestingly, the same site accounted for the lowest total microbial biomass of 1,525 ng g^{-1} (Table 2-2), indicating that higher organic matter content supports a higher microbial population due to increased substrate quantity. The C:N ratio of soil is a critical factor influencing microbial decomposition activities. Aerts & Heil (2011) reported that C:N ratio was a predictor of litter quality and decomposability. In the present study, cropland soils had C:N ratios ranging from 5:1 to 12:1, grassland soils had C:N ratios ranging from 13:1 to 15:1, and riparian soil samples had C:N ratios ranging from 10:1 to 16:1. In a study on microbial community and activity variations in agricultural ecosystems, researchers observed microbial community

activities were differentiated by soil C:N ratios (Xu et al., 2020). C:N ratio ranges from 12 to 35 in highly decomposed peat and 50 to 100 in weakly decomposed peat soils (Klemedtsson et al., 2005) whereas the studies showed C:N ratio has a negative relationship with soil CO_2 efflux (Mu et al., 2014)

Soil physical properties examined in this study included bulk density, porosity, and effective saturation (Table 2-4 and Table 2-5). Among the studied sites, the highest bulk density of 1.49 g cm^{-3} (SD = 0.06 g cm^{-3}) was observed in cropland in site 5. Overall, bulk density ranged from 1.15 to 1.49 g cm^{-3} in croplands, 0.86 to 1.10 g cm^{-3} in riparian areas, and 0.90 to 1.28 g cm^{-3} in grasslands. The lowest porosity value of 0.44 was observed in cropland of site 5, while the highest porosity value of 0.68 was observed in the riparian area of site 7, which agrees with bulk density observations. Mean bulk density between land covers was significantly different (P<0.05) with values of 1.35 g cm^{-3} in croplands, 1.13 g cm^{-3} in grasslands, and 1.00 g cm^{-3} in riparian areas. Similarly, soil porosity was also significantly different (P=0.001) across land covers, with values of 0.49 in croplands, 0.58 in grasslands, and 0.62 in riparian areas. Higher bulk densities and lower porosities in croplands could be explained by soil compaction caused by agricultural machinery and tillage. Riparian areas accounted for the lowest bulk densities, likely associated to high organic matter contents, better soil structure, and dense and proliferated root networks. Similar findings have been observed in a previous study investigating the effect of different land uses such as grasslands, cultivated lands, plantation forests, and natural forests on soil properties in northwestern Ethiopia (Selassie & Ayanna, 2013). The potential effect of these favorable conditions to soil microbial activities was reflected by R_h observations.

Soil microbial community and composition variation across sites and land covers

Soil microbial population and community composition play a crucial role in SOM decomposition and nutrient cycling. Soil microbial community composition is susceptible to soil physical and chemical properties and management practices (Xue et al., 2008). Across all studied sites and land covers, bacteria were the most dominant organisms, which is supported by the low C:N ratios (Table 2-3). Gram (+) bacteria were the most dominant microbial population closely followed by Gram (-) bacteria, which dominated in three riparian sites and one cropland site. Gram (+) bacteria typically dominate in environments that exhibit lack of soil moisture and high soil temperatures or sometimes also dominate in microbial populations coming out of winter dormancy, which aligned well with both late July and early March samplings, respectively. On the other hand, Gram (-) bacteria are common in environments with high substrate availability (e.g., low C:N ratio), in anaerobic conditions, or soils with pesticides or heavy metals which could be a possibility in cultivated soils (Fierer et al., 2003). Regarding other community groups, all the soils had <1% protozoa in terms of total microbial biomass, indicating possible lower base nutrient levels that support a high predator community. A possible reason for variations in microbial biomass and microbial composition within the same land cover category could be different litter qualities and root exudates depending on the vegetation composition (Chandra et al., 2016). Based on the results of the PLFA analysis (Table 2-2), only total microbial biomass in cropland-grassland landcover combination was statistically significant (P<0.01).

Conclusions

This study demonstrated that land cover plays an important role in R_h, with soils under cropland exhibiting a generalized lower peak and mean R_h values than soils dominated

by grassland and riparian land cover types. These differences were mainly attributed to variations in soil physical and chemical properties, including organic matter content, pH, bulk density, and total microbial biomass. Across all soil samples, peak R_h consistently occurred at WFP of 0.8 and matric potentials within the range of -4.4 to -13.3 kPa, which closely matches the typical definition of field capacity (i.e., -10 kPa). Our study demonstrates that coupling mini-precision tensiometers with simultaneous measurements of soil CO_2 efflux can effectively capture the salient R_h dynamics of undisturbed soil samples, which represents a step forward to characterizing unique R_h signatures across land covers than using disturbed soil samples and a substantial improvement over measuring R_h at a limited number of matric potentials using traditional pressure plates apparatus. The technique proposed in this study should be useful to identify better meaningful relationships between heterotrophic soil respiration and soil moisture conditions.

References

Aerts, R., & Heil, G. W. (Eds.). (2013). Heathlands: Patterns and processes in a changing environment (Vol. 20). Springer Science & Business Media.

Andraski, B. J., & Scanlon, B. R. (2018). 3.2.3 Thermocouple psychrometry. In J. H. Dane & G. Clarke Topp (Eds.), *SSSA Book Series* (pp. 609–642). Soil Science Society of America. https://doi.org/10.2136/sssabookser5.4.c22

Bardgett, R. D., Frankland, J. C., & Whittaker, J. B. (1993). The effects of agricultural management on the soil biota of some upland grasslands. *Agriculture, Ecosystems & Environment*, *45*(1–2), 25–45. https://doi.org/10.1016/0167-8809(93)90057-V

Bardgett, R. D., Wardle, D. A., & Yeates, G. W. (1998). Linking above-ground and below-ground interactions: How plant responses to foliar herbivory influence soil organisms. *Soil Biology and Biochemistry*, *30*(14), 1867–1878. https://doi.org/10.1016/S0038-0717(98)00069-8

Bauer, J., Weihermüller, L., Huisman, J. A., Herbst, M., Graf, A., Séquaris, J. M., & Vereecken, H. (2012). Inverse determination of heterotrophic soil respiration response to temperature and water content under field conditions. *Biogeochemistry*, *108*(1–3), 119–134. https://doi.org/10.1007/s10533-011-9583-1

Bradford, M. A., Davies, C. A., Frey, S. D., Maddox, T. R., Melillo, J. M., Mohan, J. E., Reynolds, J. F., Treseder, K. K., & Wallenstein, M. D. (2008). Thermal adaptation of soil microbial respiration to elevated temperature. *Ecology Letters*, *11*(12), 1316–1327. https://doi.org/10.1111/j.1461-0248.2008.01251.x

Bremer, D. J., Ham, J. M., Owensby, C. E., & Knapp, A. K. (1998). Responses of soil respiration to clipping and grazing in a tallgrass prairie. *Journal of Environmental Quality*, *27*(6), 1539–1548. https://doi.org/10.2134/jeq1998.00472425002700060034x

Chandra, L. R., Gupta, S., Pande, V., & Singh, N. (2016). Impact of forest vegetation on soil characteristics: A correlation between soil biological and physico-chemical properties. *3 Biotech*, *6*(2), 188. https://doi.org/10.1007/s13205-016-0510-y

Christensen, T. R., Jonasson, S., Callaghan, T. V., & Havström, M. (1999). On the potential CO_2 release from tundra soils in a changing climate. *Applied Soil Ecology*, *11*(2–3), 127–134. https://doi.org/10.1016/S0929-1393(98)00146-2

Ciocca, F., Lunati, I., & Parlange, M. B. (2014). Effects of the water retention curve on evaporation from arid soils. *Geophysical Research Letters*, *41*(9), 3110–3116. https://doi.org/10.1002/2014GL059827

Conant, R. T., Dalla-Betta, P., Klopatek, C. C., & Klopatek, J. M. (2004). Controls on soil respiration in semiarid soils. *Soil Biology and Biochemistry*, *36*(6), 945–951. https://doi.org/10.1016/j.soilbio.2004.02.013

Cook, F. J., & Orchard, V. A. (2008). Relationships between soil respiration and soil moisture. *Soil Biology and Biochemistry*, *40*(5), 1013–1018. https://doi.org/10.1016/j.soilbio.2007.12.012

Cox, P. M., Betts, R. A., Jones, C. D., Spall, S. A., & Totterdell, I. J. (2000). Acceleration of global warming due to carbon-cycle feedbacks in a coupled climate model. *Nature*, *408*(6809), 184–187. https://doi.org/10.1038/35041539

Curiel Yuste, J., Baldocchi, D. D., Gershenson, A., Goldstein, A., Misson, L., & Wong, S. (2007). Microbial soil respiration and its dependency on carbon inputs, soil temperature and moisture. *Global Change Biology*, *13*(9), 2018–2035. https://doi.org/10.1111/j.1365-2486.2007.01415.x

Davidson, E. A., & Janssens, I. A. (2006a). Temperature sensitivity of soil carbon decomposition and feedbacks to climate change. *Nature*, *440*(7081), 165–173. https://doi.org/10.1038/nature04514

Davidson, E. A., & Janssens, I. A. (2006b). Temperature sensitivity of soil carbon decomposition and feedbacks to climate change. *Nature*, *440*(7081), 165–173. https://doi.org/10.1038/nature04514

Davidson, EriC. A., Belk, E., & Boone, R. D. (1998). Soil water content and temperature as independent or confounded factors controlling soil respiration in a temperate mixed hardwood forest. *Global Change Biology*, *4*(2), 217–227. https://doi.org/10.1046/j.1365-2486.1998.00128.x

Eliasson, P. E., McMurtrie, R. E., Pepper, D. A., Strömgren, M., Linder, S., & Ågren, G. I. (2005). The response of heterotrophic CO_2 flux to soil warming. *Global Change Biology*, *11*(1), 167–181. https://doi.org/10.1111/j.1365-2486.2004.00878.x

Fang, C., & Moncrieff, J. B. (2001). The dependence of soil CO_2 efflux on temperature. *Soil Biology and Biochemistry*, *33*(2), 155–165. https://doi.org/10.1016/S0038-0717(00)00125-5

Fang, H., Cheng, S., Wang, Y., Yu, G., Xu, M., Dang, X., Li, L., & Wang, L. (2014). Changes in soil heterotrophic respiration, carbon availability, and microbial function in seven forests along a climate gradient. *Ecological Research*, *29*(6), 1077–1086. https://doi.org/10.1007/s11284-014-1194-6

Fierer N, Schimel JP, Holden PA (2003) Variations in microbial community composition through two soil depth profiles. Soil Biol Biochem 167–176.

Fischer, T. (2009). Substantial rewetting phenomena on soil respiration can be observed at low water availability. *Soil Biology and Biochemistry*, *41*(7), 1577–1579. https://doi.org/10.1016/j.soilbio.2009.04.009

Franzluebbers, K., Franzluebbers, A. J., & Jawson, M. D. (2002). Environmental controls on soil and whole-ecosystem respiration from a tallgrass prairie. *Soil Science Society of America Journal*, *66*(1), 254–262. https://doi.org/10.2136/sssaj2002.2540

Friend, A. D., Arneth, A., Kiang, N. Y., Lomas, M., Ogée, J., Rödenbeck, C., Running, S. W., Santaren, J.-D., Sitch, S., Viovy, N., Ian Woodward, F., & Zaehle, S. (2007). FLUXNET and modelling the global carbon cycle. *Global Change Biology*, *13*(3), 610–633. https://doi.org/10.1111/j.1365-2486.2006.01223.x

G. Selassie, Y., & Ayanna, G. (2013). Effects of different land use systems on selected physico-chemical properties of soils in northwestern Ethiopia. *Journal of Agricultural Science*, *5*(4), p112. https://doi.org/10.5539/jas.v5n4p112

Grayston, S. J., Campbell, C. D., Bardgett, R. D., Mawdsley, J. L., Clegg, C. D., Ritz, K., Griffiths, B. S., Rodwell, J. S., Edwards, S. J., Davies, W. J., Elston, D. J., & Millard, P. (2004). Assessing shifts in microbial community structure across a range of grasslands of differing management intensity using CLPP, PLFA and community DNA techniques. *Applied Soil Ecology*, *25*(1), 63–84. https://doi.org/10.1016/S0929-1393(03)00098-2

Grayston, S. J., Griffith, G. S., Mawdsley, J. L., Campbell, C. D., & Bardgett, R. D. (2001). Accounting for variability in soil microbial communities of temperate upland grassland ecosystems. *Soil Biology and Biochemistry*, *33*(4–5), 533–551. https://doi.org/10.1016/S0038-0717(00)00194-2

Guimberteau, M., Zhu, D., Maignan, F., Huang, Y., Yue, C., Dantec-Nédélec, S., Ottlé, C., Jornet-Puig, A., Bastos, A., Laurent, P., Goll, D., Bowring, S., Chang, J., Guenet, B., Tifafi, M., Peng, S., Krinner, G., Ducharne, A., Wang, F., … Ciais, P. (2018). ORCHIDEE-MICT (v8.4.1), A land surface model for the high latitudes: Model description and validation. *Geoscientific Model Development*, *11*(1), 121–163. https://doi.org/10.5194/gmd-11-121-2018

Gulledge, J., & Schimel, J. P. (1998). Moisture control over atmospheric CH_4 consumption and CO_2 production in diverse Alaskan soils. *Soil Biology and Biochemistry*, *30*(8–9), 1127–1132. https://doi.org/10.1016/S0038-0717(97)00209-5

Hamdi, S., Chevallier, T., Ben Aïssa, N., Ben Hammouda, M., Gallali, T., Chotte, J.-L., & Bernoux, M. (2011). Short-term temperature dependence of heterotrophic soil respiration after one-month of pre-incubation at different temperatures. *Soil Biology and Biochemistry*, *43*(9), 1752–1758. https://doi.org/10.1016/j.soilbio.2010.05.025

Hartley, I. P., Heinemeyer, A., & Ineson, P. (2007). Effects of three years of soil warming and shading on the rate of soil respiration: Substrate availability and not thermal acclimation mediates observed response. *Global Change Biology*, *13*(8), 1761–1770. https://doi.org/10.1111/j.1365-2486.2007.01373.x

Hartley, I. P., Hopkins, D. W., Garnett, M. H., Sommerkorn, M., & Wookey, P. A. (2008). Soil microbial respiration in arctic soil does not acclimate to temperature. *Ecology Letters*, *11*(10), 1092–1100. https://doi.org/10.1111/j.1461-0248.2008.01223.x

Hobbie, S. E., Schimel, J. P., Trumbore, S. E., & Randerson, J. R. (2000). Controls over carbon storage and turnover in high-latitude soils. *Global Change Biology*, *6*(S1), 196–210. https://doi.org/10.1046/j.1365-2486.2000.06021.x

Hui, D., & Luo, Y. (2004). Evaluation of soil CO_2 production and transport in Duke Forest using a process-based modeling approach. *Global Biogeochemical Cycles*, *18*(4), 2004GB002297. https://doi.org/10.1029/2004GB002297

Hursh, A., Ballantyne, A., Cooper, L., Maneta, M., Kimball, J., & Watts, J. (2017). The sensitivity of soil respiration to soil temperature, moisture, and carbon supply at the global scale. *Global Change Biology*, *23*(5), 2090–2103. https://doi.org/10.1111/gcb.13489

Ilstedt, U., Nordgren, A., & Malmer, A. (2000). Optimum soil water for soil respiration before and after amendment with glucose in humid tropical acrisols and a boreal mor layer. *Soil Biology and Biochemistry*, *32*(11–12), 1591–1599. https://doi.org/10.1016/S0038-0717(00)00073-0

Jayarathne, J. R. R. N., Chamindu Deepagoda, T. K. K., Clough, T. J., Thomas, S., Elberling, B., & Smits, K. M. (2021). Effect of aggregate size distribution on soil moisture, soil-gas diffusivity, and N_2O emissions from a pasture soil. *Geoderma*, *383*, 114737. https://doi.org/10.1016/j.geoderma.2020.114737

Johnson, D. D., & Guenzi, W. D. (1963). Influence of salts on ammonium oxidation and carbon dioxide evolution from soil. *Soil Science Society of America Journal*, *27*(6), 663–666. https://doi.org/10.2136/sssaj1963.03615995002700060028x

Johnson, M. S., Couto, E. G., Pinto Jr, O. B., Milesi, J., Santos Amorim, R. S., Messias, I. A. M., & Biudes, M. S. (2013). Soil CO_2 dynamics in a tree island soil of the Pantanal: The role of soil water potential. *PLoS ONE*, *8*(6), e64874. https://doi.org/10.1371/journal.pone.0064874

Keesstra, S., Geissen, V., Mosse, K., Piiranen, S., Scudiero, E., Leistra, M., & Van Schaik, L. (2012). Soil as a filter for groundwater quality. *Current Opinion in Environmental Sustainability*, *4*(5), 507–516. https://doi.org/10.1016/j.cosust.2012.10.007

Kekane, S. (2015). A review on physico-chemical properties of soil. *International Journal of Chemical Studies*, *3*(4), 29–32.

Kirschbaum, M. U. F. (2004). Soil respiration under prolonged soil warming: Are rate reductions caused by acclimation or substrate loss? *Global Change Biology*, *10*(11), 1870–1877. https://doi.org/10.1111/j.1365-2486.2004.00852.x

Klemedtsson, L., Von Arnold, K., Weslien, P., & Gundersen, P. (2005). Soil C:N ratio as a scalar parameter to predict nitrous oxide emissions. *Global Change Biology*, *11*(7), 1142–1147. https://doi.org/10.1111/j.1365-2486.2005.00973.x

Knorr, W., Prentice, I. C., House, J. I., & Holland, E. A. (2005). Long-term sensitivity of soil carbon turnover to warming. *Nature*, *433*(7023), 298–301. https://doi.org/10.1038/nature03226

Kosugi, K. (1996). Lognormal distribution model for unsaturated soil hydraulic properties. *Water Resources Research*, *32*(9), 2697–2703. https://doi.org/10.1029/96WR01776

Kucera, C. L., & Kirkham, D. R. (1971). Soil respiration studies in tallgrass prairie in Missouri. *Ecology*, *52*(5), 912–915. https://doi.org/10.2307/1936043

Lellei-Kovács, E., Kovács-Láng, E., Botta-Dukát, Z., Kalapos, T., Emmett, B., & Beier, C. (2011). Thresholds and interactive effects of soil moisture on the temperature response of soil respiration. *European Journal of Soil Biology*, *47*(4), 247–255. https://doi.org/10.1016/j.ejsobi.2011.05.004

Lessard, R., Rochette, P., Topp, E., Pattey, E., Desjardins, R. L., & Beaumont, G. (1994). Methane and carbon dioxide fluxes from poorly drained adjacent cultivated and forest sites. *Canadian Journal of Soil Science*, *74*(2), 139–146. https://doi.org/10.4141/cjss94-021

Li, X., Guo, D., Zhang, C., Niu, D., Fu, H., & Wan, C. (2018). Contribution of root respiration to total soil respiration in a semi-arid grassland on the Loess Plateau, China. *Science of The Total Environment*, *627*, 1209–1217. https://doi.org/10.1016/j.scitotenv.2018.01.313

Li, Y., Xu, M., & Zou, X. (2006). Heterotrophic soil respiration in relation to environmental factors and microbial biomass in two wet tropical forests. *Plant and Soil*, *281*(1–2), 193–201. https://doi.org/10.1007/s11104-005-4249-1

Linn, D. M., & Doran, J. W. (1984). Effect of water-filled pore space on carbon dioxide and nitrous oxide production in tilled and non-tilled soils. *Soil Science Society of America Journal*, *48*(6), 1267–1272. https://doi.org/10.2136/sssaj1984.03615995004800060013x

Lloyd, J., & Taylor, J. A. (1994). On the temperature dependence of soil respiration. *Functional Ecology*, *8*(3), 315. https://doi.org/10.2307/2389824

Luo, Y., Wan, S., Hui, D., & Wallace, L. L. (2001). Acclimatization of soil respiration to warming in a tall grass prairie. *Nature*, *413*(6856), 622–625. https://doi.org/10.1038/35098065

Manzoni, S., Schimel, J. P., & Porporato, A. (2012). Responses of soil microbial communities to water stress: Results from a meta-analysis. *Ecology*, *93*(4), 930–938. https://doi.org/10.1890/11-0026.1

Martin, J. G., & Bolstad, P. V. (2005). Annual soil respiration in broadleaf forests of northern Wisconsin: Influence of moisture and site biological, chemical, and physical characteristics. *Biogeochemistry*, *73*(1), 149–182. https://doi.org/10.1007/s10533-004-5166-8

Meyer, N., Welp, G., & Amelung, W. (2019). Effect of sieving and sample storage on soil respiration and its temperature sensitivity (Q10) in mineral soils from Germany. *Biology and Fertility of Soils*, *55*(8), 825–832. https://doi.org/10.1007/s00374-019-01374-7

Moyano, F. E., Manzoni, S., & Chenu, C. (2013). Responses of soil heterotrophic respiration to moisture availability: An exploration of processes and models. *Soil Biology and Biochemistry*, *59*, 72–85. https://doi.org/10.1016/j.soilbio.2013.01.002

Mu, Z., Huang, A., Ni, J., & Xie, D. (2014). Linking annual N_2O emission in organic soils to mineral nitrogen input as estimated by heterotrophic respiration and soil C/N ratio. *PLoS ONE*, *9*(5), e96572. https://doi.org/10.1371/journal.pone.0096572

Nakas, J. P., & Klein, D. A. (1979). Decomposition of microbial cell components in a semi-arid grassland soil. *Applied and Environmental Microbiology*, *38*(3), 454–460. https://doi.org/10.1128/aem.38.3.454-460.1979

Neff, J. C., & Hooper, D. U. (2002). Vegetation and climate controls on potential CO_2, DOC and DON production in northern latitude soils: Climate and vegetation controls over soil organic matter dynamics. *Global Change Biology*, *8*(9), 872–884. https://doi.org/10.1046/j.1365-2486.2002.00517.x

Nielsen, D. R., Th. Van Genuchten, M., & Biggar, J. W. (1986). Water flow and solute transport processes in the unsaturated zone. *Water Resources Research*, *22*(9S). https://doi.org/10.1029/WR022i09Sp0089S

Novick, K. A., Ficklin, D. L., Baldocchi, D., Davis, K. J., Ghezzehei, T. A., Konings, A. G., MacBean, N., Raoult, N., Scott, R. L., Shi, Y., Sulman, B. N., & Wood, J. D. (2022). Confronting the water potential information gap. *Nature Geoscience*, *15*(3), 158–164. https://doi.org/10.1038/s41561-022-00909-2

Orchard, V. A., & Cook, F. J. (1983). Relationship between soil respiration and soil moisture. *Soil Biology and Biochemistry*, *15*(4), 447–453. https://doi.org/10.1016/0038-0717(83)90010-X

Parker, N., Kluitenberg, G. J., Redmond, C., & Patrignani, A. (2022). A database of soil physical properties for the Kansas Mesonet. *Soil Science Society of America Journal*, *86*(6), 1495–1508. https://doi.org/10.1002/saj2.20465

Pečan, U., Pintar, M., Mihelič, R., & Kastelec, D. (2023). Variability of in situ soil water retention curves under different tillage systems and growing seasons. *Soil and Tillage Research*, *233*, 105779. https://doi.org/10.1016/j.still.2023.105779

Peel, M. C., Finlayson, B. L., & McMahon, T. A. (2007). Updated world map of the Köppen-Geiger climate classification. *Hydrology and Earth System Sciences*, *11*(5), 1633–1644. https://doi.org/10.5194/hess-11-1633-2007

Pollacco, J. A. P., Webb, T., McNeill, S., Hu, W., Carrick, S., Hewitt, A., & Lilburne, L. (2017). Saturated hydraulic conductivity model computed from bimodal water retention curves for a range of New Zealand soils. *Hydrology and Earth System Sciences*, *21*(6), 2725–2737. https://doi.org/10.5194/hess-21-2725-2017

Priha, O., Grayston, S. J., Hiukka, R., Pennanen, T., & Smolander, A. (2001). Microbial community structure and characteristics of the organic matter in soils under *Pinus sylvestris*, *Picea abi*es and *Betula pendula* at two forest sites. *Biology and Fertility of Soils*, *33*(1), 17–24. https://doi.org/10.1007/s003740000281

Pumpanen, J., Ilvesniemi, H., & Hari, P. (2003). A process-based model for predicting soil carbon dioxide efflux and concentration. *Soil Science Society of America Journal*, *67*(2), 402–413. https://doi.org/10.2136/sssaj2003.4020

Raich, J. W., & Schlesinger, W. H. (1992). The global carbon dioxide flux in soil respiration and its relationship to vegetation and climate. *Tellus B*, *44*(2), 81–99. https://doi.org/10.1034/j.1600-0889.1992.t01-1-00001.x

Raich, J. W., & Tufekciogul, A. (2000a). Vegetation and soil respiration: Correlations and controls. *Biogeochemistry*, *48*(1), 71–90. https://doi.org/10.1023/A:1006112000616

Reichstein, M., Rey, A., Freibauer, A., Tenhunen, J., Valentini, R., Banza, J., Casals, P., Cheng, Y., Grünzweig, J. M., Irvine, J., Joffre, R., Law, B. E., Loustau, D., Miglietta, F., Oechel, W., Ourcival, J., Pereira, J. S., Peressotti, A., Ponti, F., … Yakir, D.

(2003). Modeling temporal and large-scale spatial variability of soil respiration from soil water availability, temperature and vegetation productivity indices. *Global Biogeochemical Cycles*, *17*(4), 2003GB002035. https://doi.org/10.1029/2003GB002035

Reichstein, M., Subke, J., Angeli, A. C., & Tenhunen, J. D. (2005). Does the temperature sensitivity of decomposition of soil organic matter depend upon water content, soil horizon, or incubation time? *Global Change Biology*, *11*(10), 1754–1767. https://doi.org/10.1111/j.1365-2486.2005.001010.x

Rodeghiero, M., & Cescatti, A. (2005). Main determinants of forest soil respiration along an elevation/temperature gradient in the Italian Alps. *Global Change Biology*, *11*(7), 1024–1041. https://doi.org/10.1111/j.1365-2486.2005.00963.x

Schimel, J. P., Gulledge, J. M., Clein-Curley, J. S., Lindstrom, J. E., & Braddock, J. F. (1999). Moisture effects on microbial activity and community structure in decomposing birch litter in the Alaskan taiga. *Soil Biology and Biochemistry*, *31*(6), 831–838. https://doi.org/10.1016/S0038-0717(98)00182-5

Schindlbacher, A., Zechmeister-Boltenstern, S., & Jandl, R. (2009). Carbon losses due to soil warming: Do autotrophic and heterotrophic soil respiration respond equally? *Global Change Biology*, *15*(4), 901–913. https://doi.org/10.1111/j.1365-2486.2008.01757.x

Schindler, U., & Müller, L. (2006). Simplifying the evaporation method for quantifying soil hydraulic properties. *Journal of Plant Nutrition and Soil Science*, *169*(5), 623–629. https://doi.org/10.1002/jpln.200521895

Schnürer, J., Clarholm, M., Boström, S., & Rosswall, T. (1986). Effects of moisture on soil microorganisms and nematodes: A field experiment. *Microbial Ecology*, *12*(2), 217–230. https://doi.org/10.1007/BF02011206

Shaver, G. R., Canadell, J., Chapin, F. S., Gurevitch, J., Harte, J., Henry, G., Ineson, P., Jonasson, S., Melillo, J., Pitelka, L., & Rustad, L. (2000). Global warming and terrestrial ecosystems: A conceptual framework for analysis. *BioScience*, *50*(10), 871. https://doi.org/10.1641/0006-3568(2000)050[0871:GWATEA]2.0.CO;2

Singh, B. R., Agarwal, A. S., & Kanehiro, Y. (1969). Effect of chloride salts on ammonium nitrogen release in two Hawaiian soils. *Soil Science Society of America Journal*, *33*(4), 557–560. https://doi.org/10.2136/sssaj1969.03615995003300040021x

Stocker, T. (Ed.). (2014). *Climate change 2013: The physical science basis: Working Group I contribution to the Fifth assessment report of the Intergovernmental Panel on Climate Change*. Cambridge University Press.

Striegl, R. G., & Wickland, K. P. (1998). Effects of a clear-cut harvest on soil respiration in a jack pine—Lichen woodland. *Canadian Journal of Forest Research*, *28*(4), 534–539. https://doi.org/10.1139/x98-023

Torbert, H. A., & Wood, C. W. (1992). Effects of soil compaction and water-filled pore space on soil microbial activity and N losses. *Communications in Soil Science and Plant Analysis*, *23*(11–12), 1321–1331. https://doi.org/10.1080/00103629209368668

Towne, E. G. (2002). Vascular plants of Konza prairie biological station: An annotated checklist of species in a kansas tallgrass prairie. *SIDA, Contributions to Botany*, *20*(1), 269–294.

Tufekcioglu, A., Raich, J. W., Isenhart, T. M., & Schultz, R. C. (2001). Soil respiration within riparian buffers and adjacent crop fields. *Plant and Soil*, *229*(1), 117–124. https://doi.org/10.1023/A:1004818422908

Van Genuchten, M. Th. (1980). A closed-form equation for predicting the hydraulic conductivity of unsaturated soils. *Soil Science Society of America Journal*, *44*(5), 892–898. https://doi.org/10.2136/sssaj1980.03615995004400050002x

Whalley, W. R., Ober, E. S., & Jenkins, M. (2013). Measurement of the matric potential of soil water in the rhizosphere. *Journal of Experimental Botany*, *64*(13), 3951–3963. https://doi.org/10.1093/jxb/ert044

Wickland, K. P., & Neff, J. C. (2008). Decomposition of soil organic matter from boreal black spruce forest: Environmental and chemical controls. *Biogeochemistry*, *87*(1), 29–47. https://doi.org/10.1007/s10533-007-9166-3

Xu, Z., Zhang, T., Wang, S., & Wang, Z. (2020). Soil pH and C/N ratio determines spatial variations in soil microbial communities and enzymatic activities of the agricultural ecosystems in Northeast China: Jilin Province case. *Applied Soil Ecology*, *155*, 103629. https://doi.org/10.1016/j.apsoil.2020.103629

Xue, D., Yao, H.-Y., Ge, D.-Y., & Huang, C.-Y. (2008). Soil microbial community structure in diverse land use systems: A comparative study using Biolog, DGGE, and PLFA analyses. *Pedosphere*, *18*(5), 653–663. https://doi.org/10.1016/S1002-0160(08)60060-0

Yan, Z., Liu, C., Todd-Brown, K. E., Liu, Y., Bond-Lamberty, B., & Bailey, V. L. (2016). Pore-scale investigation on the response of heterotrophic respiration to moisture conditions in heterogeneous soils. *Biogeochemistry*, *131*(1–2), 121–134. https://doi.org/10.1007/s10533-016-0270-0

Zhang, W., Parker, K. M., Luo, Y., Wan, S., Wallace, L. L., & Hu, S. (2005). Soil microbial responses to experimental warming and clipping in a tallgrass prairie. *Global Change Biology*, *11*(2), 266–277. https://doi.org/10.1111/j.1365-2486.2005.00902.x

Zhou, W., Hui, D., & Shen, W. (2014). Effects of soil moisture on the temperature sensitivity of soil heterotrophic respiration: A laboratory incubation study. *PLoS ONE*, *9*(3), e92531. https://doi.org/10.1371/journal.pone.0092531

Zogg, G. P., Zak, D. R., Ringelberg, D. B., White, D. C., MacDonald, N. W., & Pregitzer, K. S. (1997). Compositional and functional shifts in microbial communities due to soil warming. *Soil Science Society of America Journal*, *61*(2), 475–481. https://doi.org/10.2136/sssaj1997.03615995006100020015x

Table 2-1: Location, geographic coordinates, land cover type, dominant vegetation type, and dominant soil series data for the locations sampled in this study.

Site	Location	Coordinates	Land use/land cover	Soil series†
1	Gypsum	38.71302 N, 97.42108 W	Cropland. Fallow with winter wheat residue	Cozad
1	Gypsum	38.71284 N, 97.42102 W	Riparian. Honey locust, Black walnut	Cozad
2	Ashland Bottoms	39.14627 N, 96.63499 W	Cropland. Winter wheat residue	Stonehouse – Eudora complex
2	Ashland Bottoms	39.14633 N, 96.63587 W	Riparian. Honey locust	Stonehouse – Eudora complex
3	Moundridge	38.21030 N, 97.56956 W	Cropland. Standing winter wheat	Crete
3	Moundridge	38.21047 N, 97.56958 W	Riparian. Eastern cottonwood, Honey locust	Crete
4	Konza Prairie	39.10622 N, 96.61045 W	Cropland. Corn residue	Reading
4	Konza Prairie	39.10595 N, 96.61060 W	Grassland. Tallgrass	Reading
5	Konza Prairie	39.10390 N, 96.60730 W	Cropland. Standing soybean	Reading
5	Konza Prairie	39.10324 N, 96.60720 W	Grassland. Tallgrass and herbaceous plants	Reading
6	Ashland Bottoms	39.13022 N, 96.64411 W	Cropland. Standing corn	Smolan
6	Ashland Bottoms	39.13070 N, 96.64354 W	Grassland. Tallgrass	Smolan
7	Konza Prairie	39.10180 N, 96.59841 W	Grassland. Indian grass, Little bluestem	Ivan
7	Konza Prairie	39.10216 N, 96.59834 W	Riparian. Bur oak, Black walnut	Ivan
8	Konza Prairie	39.10256 N, 96.58228 W	Grassland. Indian grass, Little bluestem	Ivan
8	Konza Prairie	39.10218 N, 96.58232 W	Riparian. Bur oak, Black walnut	Ivan

9	Konza Prairie	39.09623 N, 96.58977 W	Grassland. Indian grass, Little bluestem	Tully
9	Konza Prairie	39.09600 N, 96.58896 W	Riparian. Bur oak, Black walnut	Tully

† According to the USDA-NRCS web Soil Survey

Table 2-2: Total bacteria biomass, Gram (+) bacteria, Gram (-) bacteria, total fungi biomass, and total protozoa biomass for each site and land cover type using the Phospholipid Fatty Acid (PLFA) analysis. Numbers within parentheses indicate the percentage of each microbial community in total microbial biomass. The difference between the total microbial biomass and the summation of total bacteria, total fungi, and protozoa represents undifferentiated microbial biomass (values not reported).

Site	Land cover	Bacteria	Gram (+)	Gram (-)	Fungi	Protozoa	Total biomass
		ng g^{-1}	ng g^{-1}	ng g^{-1}	ng g^{-1}	ng g^{-1}	ng g^{-1}
1	Cropland	1308 (36)	684 (19)	624 (17.1)	706 (19.5)	5 (0.1)	3628
1	Riparian	2369 (49)	1063 (21.9)	1306 (26.9)	788 (16.2)	3 (0.1)	4850
2	Cropland	573 (38)	347 (22.7)	226 (14.8)	207 (13.6)	0	1525
2	Riparian	1388 (49)	659 (23.0)	729 (25.4)	392 (13.7)	0	2865
3	Cropland	1085 (37.5)	494 (17.1)	591 (20.4)	522 (18.0)	0	2894
3	Riparian	1209 (43.7)	485 (17.5)	724 (26.1)	484 (17.5)	0	2768
4	Cropland	1453 (44.3)	928 (28.3)	524 (16.0)	399 (12.2)	15 (0.5)	3280
4	Grassland	2648 (45.1)	1521 (25.9)	1127 (19.2)	1024 (17.4)	53 (0.9)	5872
5	Cropland	975 (48.6)	582 (29.0)	393 (19.6)	241 (12.0)	0	2008
5	Grassland	2377 (45.8)	1535 (29.6)	842 (16.2)	751 (14.5)	11 (0.2)	5188
6	Cropland	1519 (48.5)	910 (29.0)	610 (19.4)	423 (13.5)	11 (0.4)	3133
6	Grassland	2377 (50.0)	1351 (28.4)	1026 (21.6)	703 (14.8)	0	4752
7	Grassland	1185 (47.0)	723 (28.7)	462 (18.3)	373 (14.8)	2 (0.1)	2520
7	Riparian	1941 (53.1)	1081 (29.6)	859 (23.5)	509 (13.9)	7 (0.2)	3658
8	Grassland	4352 (47.8)	2695 (29.6)	1657 (18.2)	1167 (12.8)	14.4 (0.2)	9099
8	Riparian	5123 (53.4)	3082 (32.1)	2041 (21.3)	1220 (12.7)	17 (0.2)	9601
9	Grassland	4942 (48.4)	3443 (33.7)	1499 (14.7)	1183 (11.6)	16 (0.2)	10218
9	Riparian	4152 (50.5)	2647 (32.2)	1506 (18.3)	879 (10.7)	11 (0.1)	8218

Table 2-3: Physico-chemical properties of the soils studied including pH, EC, CEC, organic matter (OM %) by loss on ignition method, total nitrogen (Total N %), and total carbon (Total C %).

Site	Land cover	pH	EC	CEC	OM	Total N	Total C	C:N ratio
			$\mu S\ cm^{-1}$	meq per 100 g	%	%	%	
1	Cropland	6.1	272	13.4	3.3	0.19	1.78	9
1	Riparian	7.3	399	22.9	4.0	0.19	2.22	12
2	Cropland	5.8	216	5.60	1.3	0.13	0.670	5
2	Riparian	7.5	175	13.4	3.2	0.19	2.07	11
3	Cropland	5.0	551	21.4	6.2	0.30	3.48	12
3	Riparian	6.9	785	21.5	4.5	0.25	2.45	10
4	Cropland	5.6	90.1	20.4	3.4	0.18	1.77	10
4	Grassland	6.7	163	24.4	6.9	0.26	3.94	15
5	Cropland	7.2	131	24.5	3.2	0.15	1.77	12
5	Grassland	7.1	107	26.9	4.4	0.20	2.58	13
6	Cropland	6.6	85.3	19.9	6.1	0.31	3.50	11
6	Grassland	6.2	216	14.8	3.6	0.15	1.98	13
7	Grassland	7.3	314	27.0	4.8	0.21	2.65	13
7	Riparian	7.4	113	34.0	10.	0.36	5.53	15
8	Grassland	6.5	88.2	28.4	7.1	0.33	4.21	13
8	Riparian	6.2	165	31.9	9.0	0.43	6.70	16
9	Grassland	6.5	77.3	34.1	7.4	0.31	4.24	14
9	Riparian	6.5	81.1	27.9	7.5	0.34	4.44	13

Table 2-4: Soil water retention parameters for the van Genuchten model obtained for the 18 studied soils. Soil water retention curves were determined in laboratory conditions using a combination of precision mini-tensiometers (model Hyprop 2, Meter Group, Inc.) and a dew point soil water potential meter (model WP4C, Meter Group, Inc.). Values of $\theta_r < 0.001$ cm^3 cm^{-3} were recorded as 0.

Site	Land cover	α	n	θ_r	θ_s
		kPa^{-1}	Unitless	$cm^3\,cm^{-3}$	$cm^3\,cm^{-3}$
1	Cropland	0.103	1.349	0.024	0.458
1	Riparian	0.751	1.221	0	0.602
2	Cropland	0.080	2.305	0.045	0.434
2	Riparian	0.124	2.109	0.065	0.558
3	Cropland	0.254	1.310	0.028	0.506
3	Riparian	0.927	1.221	0	0.569
4	Cropland	0.511	1.184	0.015	0.493
4	Grassland	0.379	1.196	0	0.547
5	Cropland	0.120	1.184	0	0.480
5	Grassland	0.286	1.168	0	0.515
6	Cropland	0.077	1.858	0.107	0.490
6	Grassland	0.258	1.358	0.080	0.558
7	Grassland	0.367	1.174	0	0.518
7	Riparian	1.000	1.281	0.102	0.617
8	Grassland	0.158	1.301	0.116	0.491
8	Riparian	1.00	1.236	0.122	0.542
9	Grassland	1.00	1.241	0.027	0.655
9	Riparian	1.00	1.261	0.068	0.675

Table 2-5: Soil physical properties including the percentage of sand and clay fractions, average bulk density (ρ_b), mean volumetric water content at the time of sampling (θ_v), and average porosity (f). The standard deviation for the three replicates is reported in brackets.

Site	Land use	Sand	Clay	Soil textural class†	θ_v	ρ_b	f
		%	%		$cm^3\ cm^{-3}$	$g\ cm^{-3}$	
1	Cropland	33	18	Loam	0.33 (±0.01)	1.42 (±0.04)	0.47 (±0.02)
1	Riparian	23	31	Clay loam	0.28 (±0.01)	1.05 (±0.12)	0.60 (±0.05)
2	Cropland	52	8	Sandy loam	0.27 (±0.01)	1.39 (±0.05)	0.48 (±0.02)
2	Riparian	46	10	Loam	0.23 (±0.03)	1.10 (±0.10)	0.58 (±0.04)
3	Cropland	16	28	Silty clay loam	0.26 (±0.02)	1.15 (±0.11)	0.57 (±0.04)
3	Riparian	17	26	Silt loam	0.29 (±0.01)	1.04 (±0.03)	0.61 (±0.02)
4	Cropland	13	31	Silty clay loam	0.35 (±0.01)	1.33 (±0.02)	0.50 (±0.01)
4	Grassland	12	31	Silty clay loam	0.42 (±0.03)	1.07 (±0.03)	0.60 (±0.01)
5	Cropland	12	36	Silty clay loam	0.27 (±0.02)	1.49 (±0.06)	0.44 (±0.02)
5	Grassland	10	36	Silty clay loam	0.30 (±0.01)	1.28 (±0.03)	0.52 (±0.01)
6	Cropland	19	23	Silt loam	0.31 (±0.01)	1.32 (±0.06)	0.50 (±0.02)
6	Grassland	16	23	Silt loam	0.18 (±0.01)	1.03 (±0.10)	0.61 (±0.04)
7	Grassland	12	36	Silty clay loam	0.43 (±0.04)	1.28 (±0.10)	0.52 (±0.03)
7	Riparian	12	33	Silty clay loam	0.39 (±0.04)	0.86 (±0.19)	0.68 (±0.07)
8	Grassland	11	34	Silty clay loam	0.29 (±0.01)	1.20 (0.03)	0.54(±0.01)
8	Riparian	23	36	Clay loam	0.33 (±0.02)	1.09 (±0.15)	0.59 (±0.06)
9	Grassland	12	39	Silty clay loam	0.23 (±0.03)	0.90 (±0.09)	0.66 (±0.04)
9	Riparian	13	28	Silty clay loam	0.19 (±0.02)	0.91 (±0.07)	0.66 (±0.03)

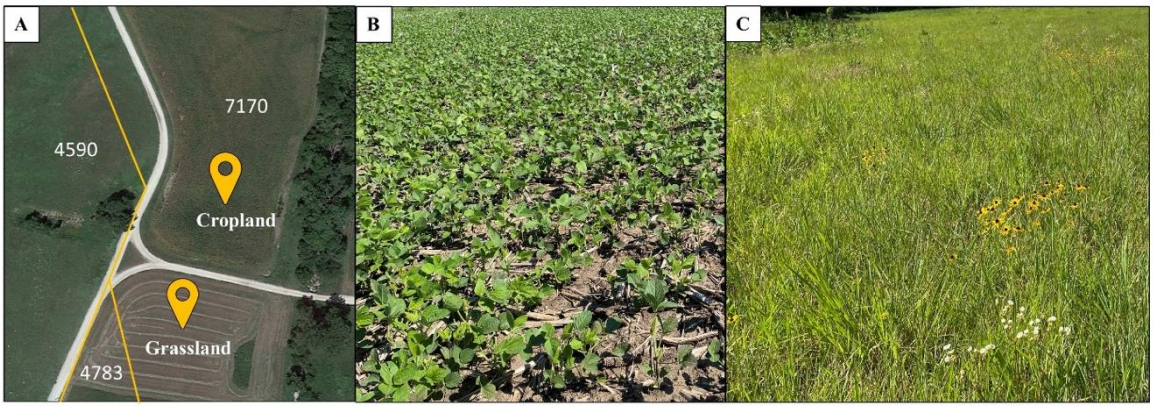

Figure 2-1: A) Satellite image (8/9/2022) showing the cropland and grassland sampling locations for one of the sites located within the Konza Prairie Biological Station near Manhattan, KS. The map also shows the soil series (yellow color lines) and map units (numbers) according to NRCS Soil Survey Geodatabase. In this site, adjacent cropland and grassland fields belonged to the Reading silt loam soil series (7170 map unit); B) example picture of the sampled cropland area with soybean at V3 leaf development stage; and C) picture of the grassland site dominated by short grasses and a few scattered forbs.

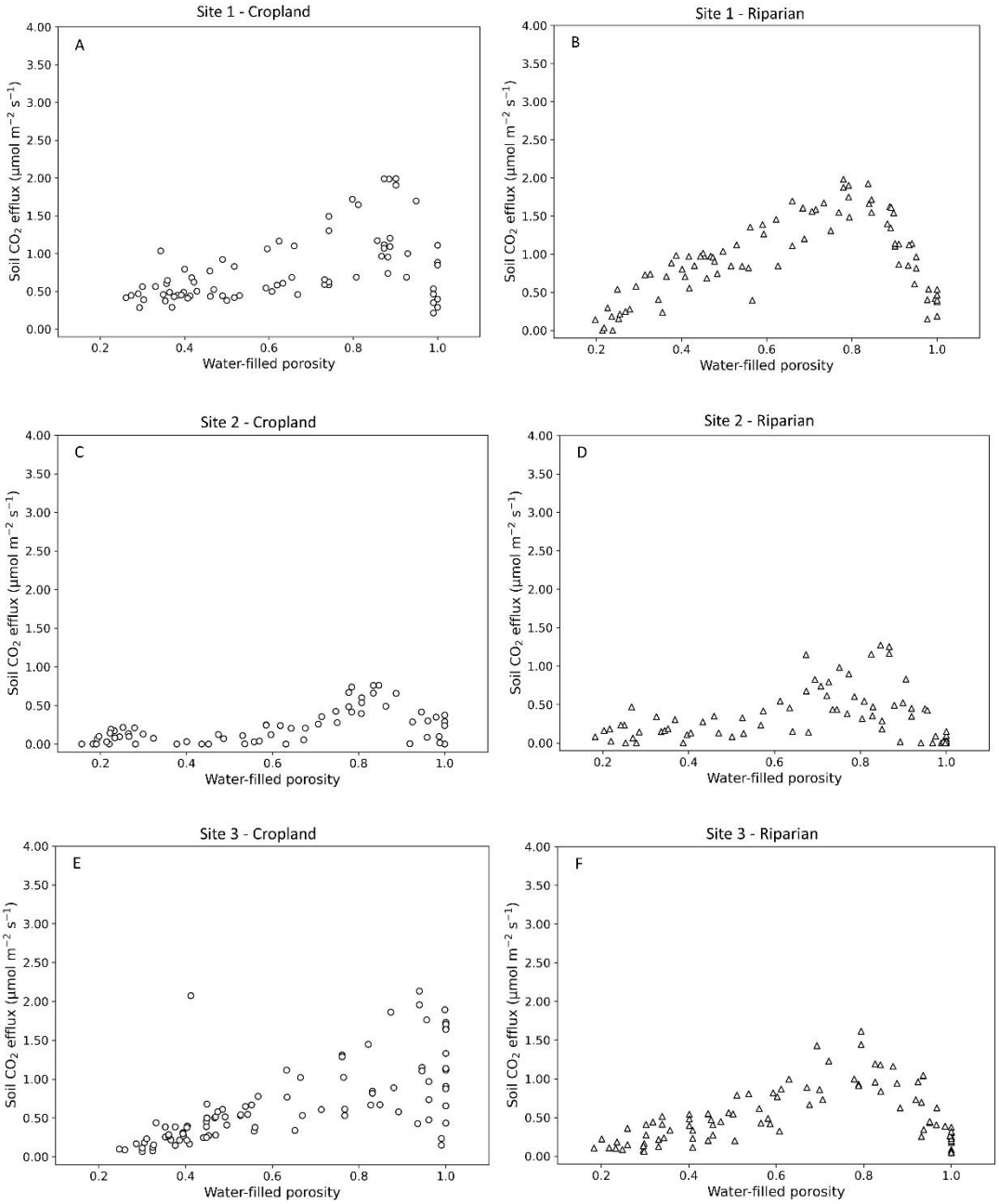

Figure 2-2: Soil CO_2 efflux as a function of water-filled porosity for undisturbed soil samples obtained from adjacent cropland-riparian land covers across three sites in central Kansas. Soil CO_2 efflux was measured manually using a gas chamber connected to an infrared gas analyzer and water-filled porosity was calculated using volumetric water contents given by Hyprop system. The measurements were conducted in laboratory conditions during a period of 10-15 days at ambient temperature and CO_2 concentration.

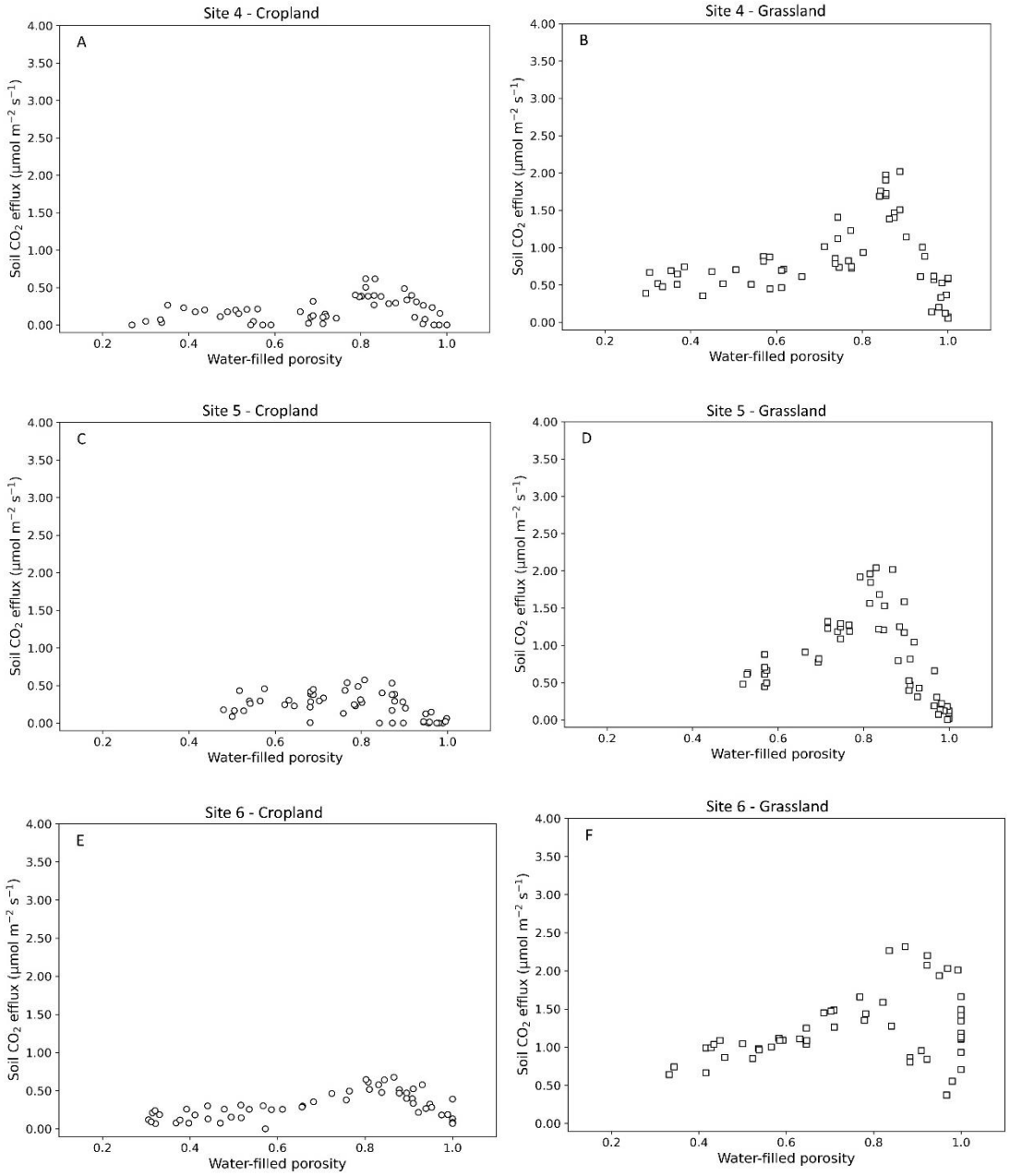

Figure 2-3: Soil CO_2 efflux as a function of water-filled porosity for undisturbed soil samples obtained from adjacent cropland-grassland land covers across three sites in central Kansas. Soil CO_2 efflux was measured manually using a gas chamber connected to an infrared gas analyzer and water-filled porosity was calculated using volumetric water contents given by Hyprop system. The measurements were conducted in laboratory conditions during a period of 10-15 days at ambient temperature and CO_2 concentration.

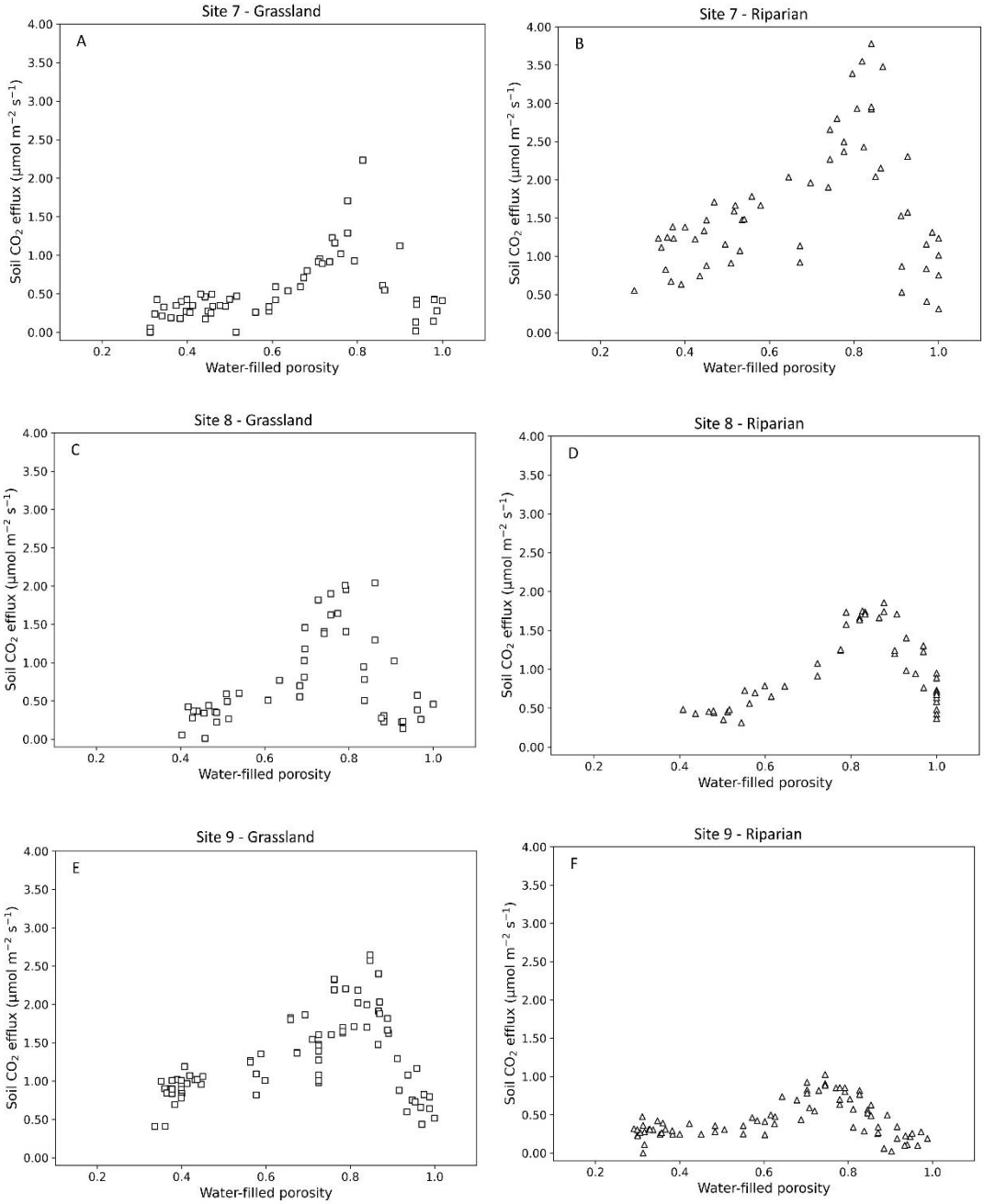

Figure 2-4: Soil CO_2 efflux as a function of water-filled porosity for undisturbed soil samples obtained from adjacent grassland-riparian land covers across three sites in central Kansas. Soil CO_2 efflux was measured manually using a gas chamber connected to an infrared gas and water-filled porosity was calculated using volumetric water contents given by Hyprop system. The measurements were conducted in laboratory conditions during a period of 10-15 days at ambient temperature and CO_2 concentration.

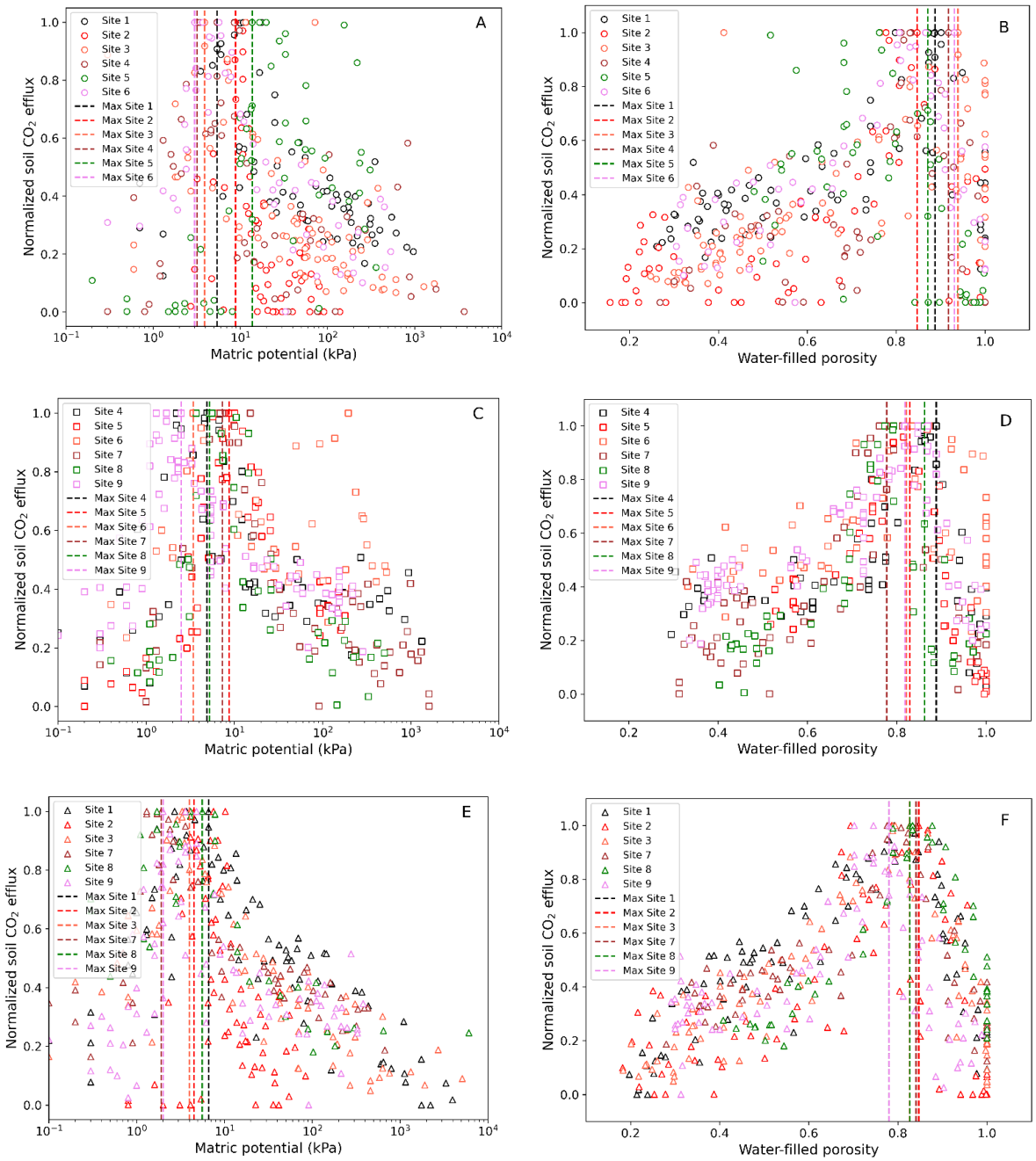

Figure 2-5: Combined relative soil CO_2 efflux as a function of A) soil matric potential and B) water-filled porosity for all undisturbed soil samples collected in cropland, grassland, and riparian areas. Vertical lines indicate the matric potential or water-filled porosity at which the maximum CO_2 efflux was observed.

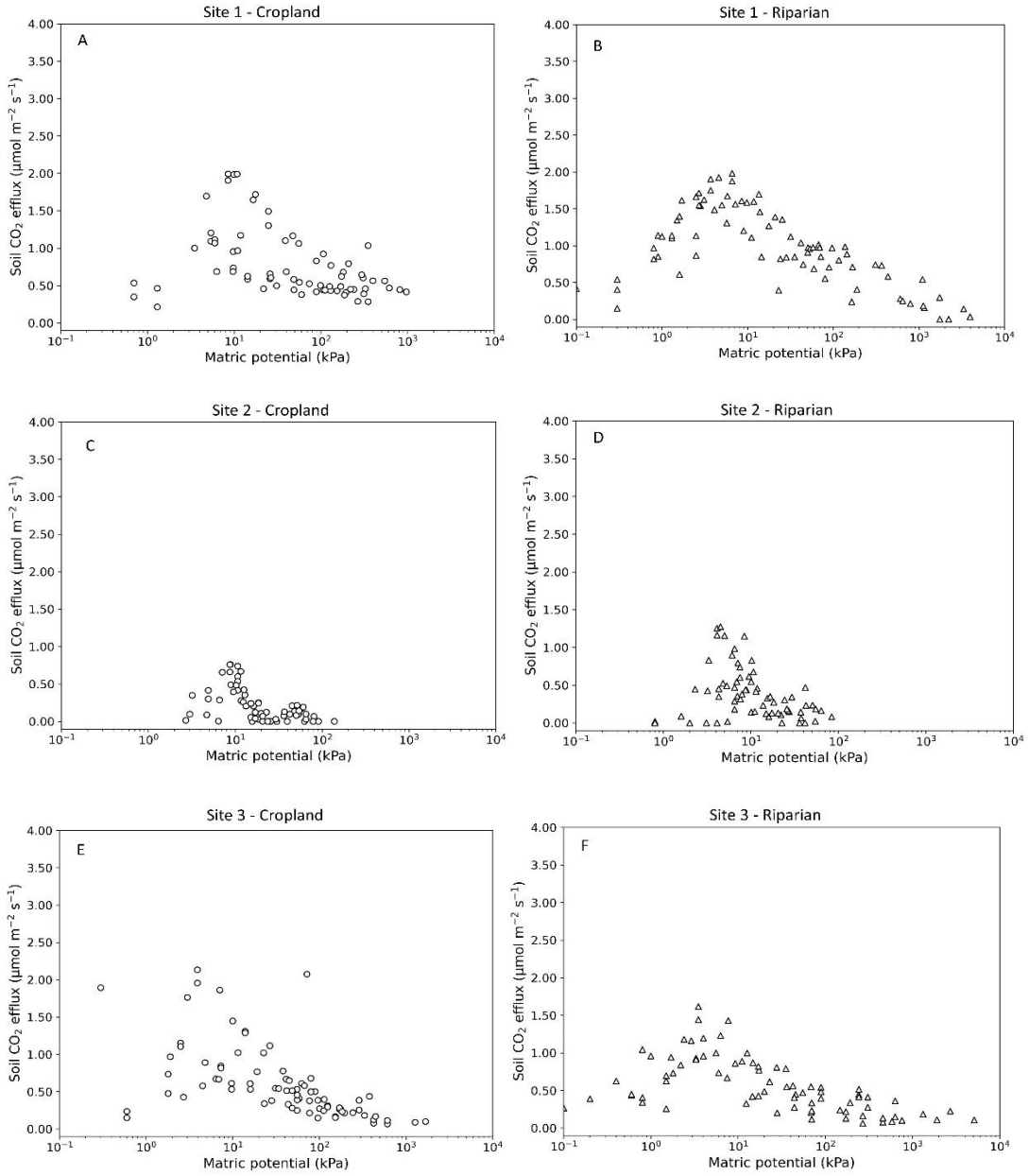

Figure 2-6: Soil CO_2 efflux as a function of soil matric potential for undisturbed soil samples obtained from adjacent cropland-riparian land covers across three sites in central Kansas. Soil CO_2 efflux was measured manually using a gas chamber connected to an infrared gas analyzer and matric potential was measured using precision mini-tensiometers. The curves were obtained in laboratory conditions during a period of 10-15 days at ambient temperature and CO_2 concentration.

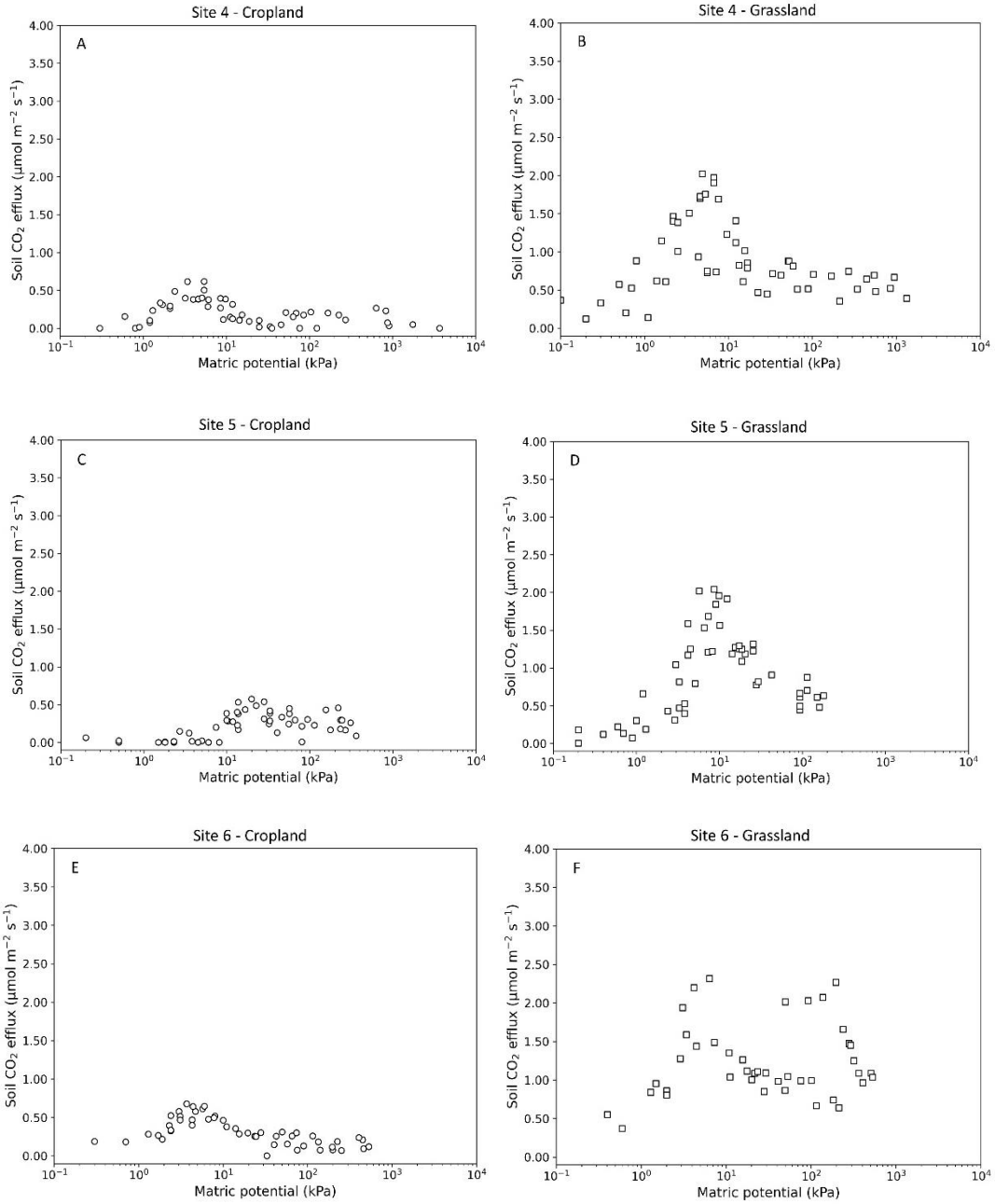

Figure 2-7: Soil CO_2 efflux as a function of soil matric potential for undisturbed soil samples obtained from adjacent cropland-grassland land covers across three sites in central Kansas. Soil CO_2 efflux was measured manually using a gas chamber connected to an infrared gas analyzer and matric potential was measured using precision mini-tensiometers. The curves were obtained in laboratory conditions during a period of 10-15 days at ambient temperature and CO_2 concentration.

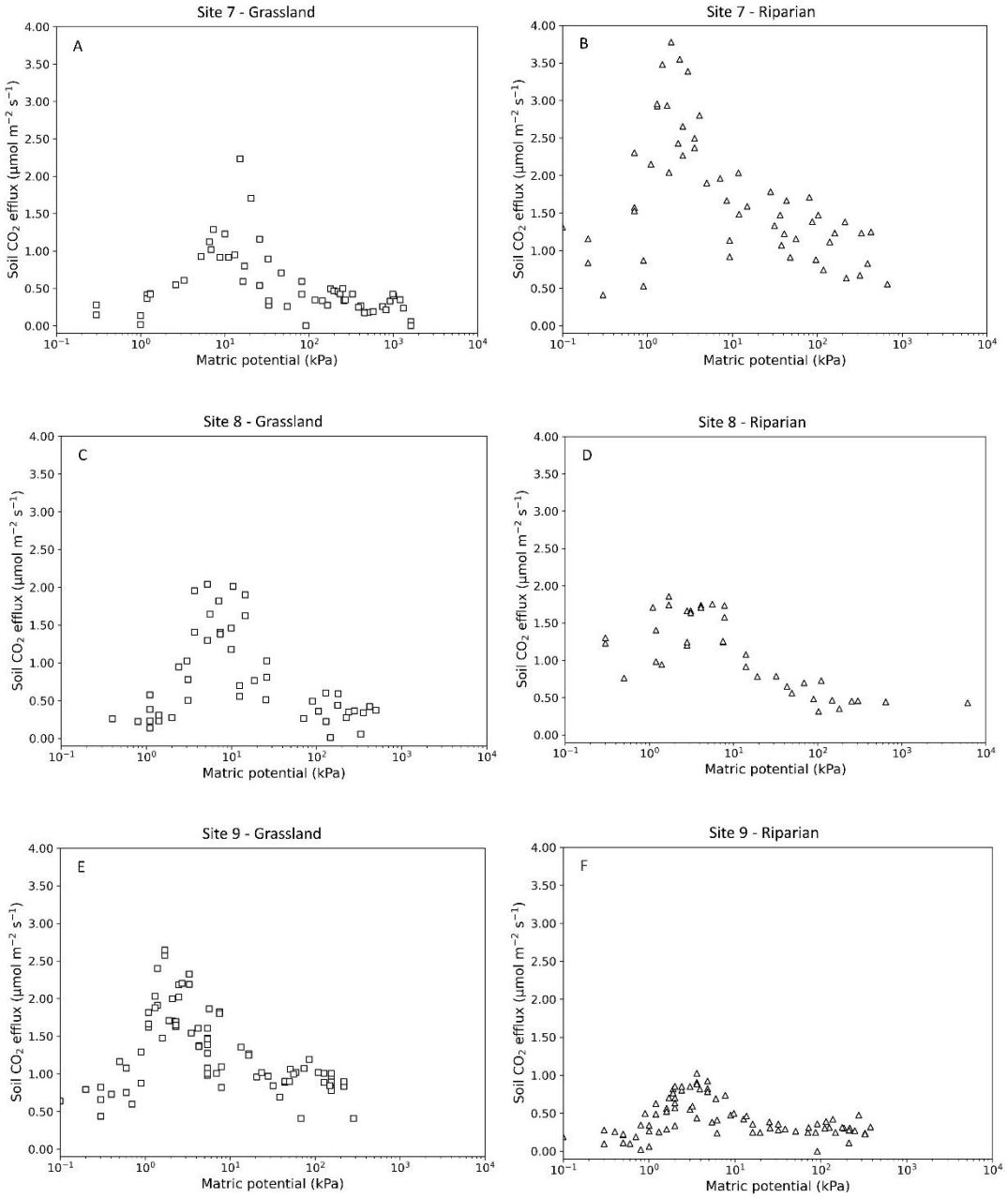

Figure 2-8: Soil CO_2 efflux as a function of soil matric potential for undisturbed soil samples obtained from adjacent grassland-riparian land covers across three sites in central Kansas. Soil CO_2 efflux was measured manually using a gas chamber connected to an infrared gas analyzer and matric potential was measured using precision mini-tensiometers. The curves were obtained in laboratory conditions during a period of 10-15 days at ambient temperature and CO_2 concentration.

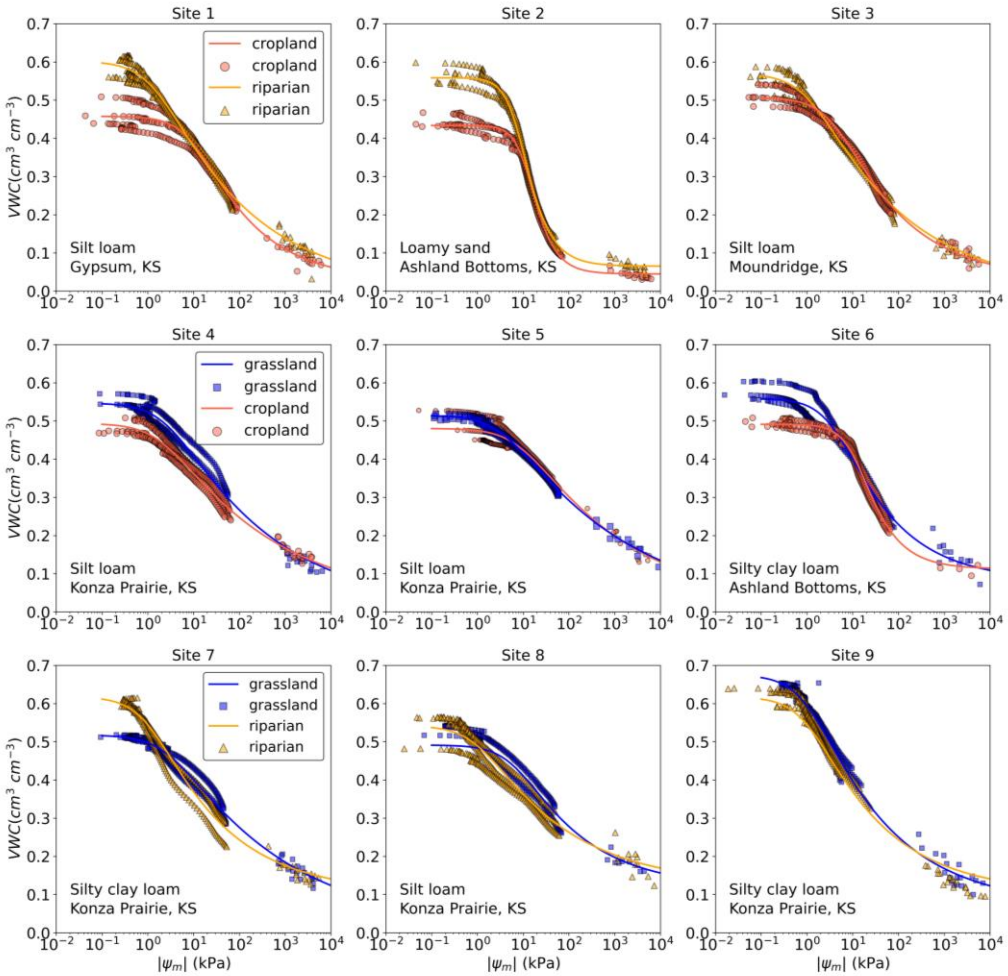

Figure 2-9: Soil water retention curves for the two land cover pairs at each site. Markers represent measurements made with precision mini-tensiometers (model Hyprop 2, Meter group) and a dew point soil water potential meter (model WP4C, Meter group). Lines represent the fitted van Genuchten model for each land cover.

Chapter 3 - Coupling *In Situ* Soil Water Retention Curves with Soil Respiration Measurements to Study Heterotrophic Soil Respiration Dynamics in Field Conditions

Nishadini Widanagamage and Andres Patrignani

Abstract

Heterotrophic soil respiration (R_h) represents the release of carbon dioxide (CO_2) from the soil due to microbial and faunal respiration. Understanding how R_h responds to environmental factors is crucial for predicting soil carbon dynamics and forecasting the potential impact of climate change on terrestrial carbon stocks. The objective of this study was to investigate the relationship between R_h and two key environmental factors: soil matric potential and soil temperature under field conditions. The experiment was conducted in a tallgrass prairie at the Konza Prairie Biological Station near Manhattan, KS. Six plastic collars (10 cm long and 10 cm inner diameter) were inserted into the undisturbed soil and then instrumented with matric potential, temperature, and volumetric water content sensors. Soil CO_2 efflux was measured manually using an infrared CO_2 gas analyzer four to six times per week. Soil moisture ranged from near-saturation to air-dry conditions, resulting in a wide range of soil matric potentials from -0.1 to -5,900 kPa and soil temperature at a depth of 3.5 cm varied from 15 to 50 °C. The median soil CO_2 efflux at the site was 4.40 µmol m^{-2} s^{-1}. Peak R_h of 7.10 µmol m^{-2} s^{-1} was observed at -30 kPa matric potential and 35 °C soil temperature, declining as soil matric potential became more negative. The effect of soil temperature on R_h was less pronounced at temperatures over 40 °C. According to univariate and multivariate linear regression analysis, water-filled porosity (R-square = 0.62, RMSE = 0.19 µmol m^{-2} s^{-1}) was a better predictor of R_h than soil matric potential (R-square = 0.56, RMSE = 0.20 µmol m^{-2} s^{-1}). Coupling *in situ* soil moisture retention curves with soil

respiration measurements revealed soil moisture and R_h dynamics that are challenging to observe and may go unnoticed in laboratory conditions.

Introduction

Soil organic carbon (SOC) represents the largest reservoir of terrestrial carbon (C) and is the result of the balance between carbon inputs, such as leaf and root debris, and carbon outputs, such as carbon dioxide (CO_2) and methane (CH_4) that can be released back to the atmosphere through soil respiration (R_s). In recent decades, the key role of R_s in the global carbon cycle and its potential feedback on climate change have propelled a growing interest in accurately predicting soil CO_2 efflux in response to changing environmental conditions (Novick et al., 2022). Environmental and land surface models that are used for global C storage predictions typically simulate R_s as an aggregated component that includes both heterotrophic respiration (R_h) and autotrophic respiration (R_a) (Guimberteau et al., 2018) (Friend et al., 2007). However, each component of R_s is controlled differently by environmental factors, which underline the necessity for separate consideration, to reduced model uncertainty (Conant et al., 2004; Schindlbacher et al., 2009)

The main factors influencing R_h include soil moisture (Gulledge & Schimel, 1998; Schimel et al., 1999), soil temperature (Christensen et al., 1999; Neff & Hooper, 2002), and substrate quality and availability (Hobbie et al., 2000). Although there has been an emphasis on soil microbial response to temperature (Bradford et al., 2008; Hartley et al., 2008; Zhang et al., 2005), there is need to further investigate how the combined effect of both soil moisture and soil temperature influence R_h to better understand the fate of SOC stocks, global greenhouse gas emissions, and the future composition of the atmosphere in the context of climate change (Johnson et al., 2013; Moyano et al., 2013).

Soil moisture is a state variable that highly depends on the precipitation regime, atmospheric demand, soil type, and soil hydraulic properties, which control processes such as soil evaporation (Ciocca et al., 2014), solute transport (Nielsen et al., 1986), plant water availability (Whalley et al., 2013), soil microbial activity (Manzoni et al., 2012), and gas

fluxes within and from the soil (Jayarathne et al., 2021). A soil respiration study conducted in five different forest types in north-central Wisconsin over a two-year period suggests that soil moisture is a more important limiting factor of soil respiration than soil temperature during drought periods (Martin & Bolstad, 2005). A process-based modelling study for predicting soil R_h has also found that R_h strongly depends on soil water content and ignoring soil water content leads to over estimation of R_h (Pumpanen et al., 2003). Another study conducted on the interactive effect of soil temperature and soil moisture in a sandy forest-steppe in Hungary concluded that the soil moisture has a significant effect on R_s in semiarid ecosystems (Lellei-Kovács et al., 2011).

In soil respiration studies, soil moisture is often represented using indicators on a mass or a volume basis (e.g., Li et al., 2018; Martin & Bolstad, 2005; Wickland & Neff, 2008), which are easy to determine using gravimetric methods and a wide range of sensors. However, because mass-based and volume-based soil moisture indicators do not account for the amount of work that needs to be exerted by soil microorganisms to access pore water, using volumetric or gravimetric indicators may hinder a more fundamental understanding of the relationship between soil water content and R_h. Thus, using a variable like the soil water potential, which represents the energy-state of the pore water in terms of potential energy, may be a better alternative to describe the fundamental responses of R_h and overall soil carbon fluxes across soils with different particle and pore size distributions (Orchard & Cook, 1983). Soil water potential represents the driving force of water movement in soils and plays a central role in regulating microbial activity. Despite its evident importance in ecosystem and biogeochemical processes, only a limited number of studies have considered the effect of soil water potential on R_h. Furthermore, most of these studies have been conducted under laboratory conditions using disturbed soil samples (Conant et al., 2004; Fischer, 2009; Yan et al., 2016), without accounting for repeated drying and wetting cycles, which are common in

field conditions. In this study, we hypothesize that *in situ* measurements of soil water potential better describes heterotrophic soil respiration dynamics during multiple wetting and drying events over gravimetric or volumetric soil moisture indicators. The objective of this study was to investigate the relationship between heterotrophic soil respiration and the energy-state of pore water by coupling *in situ* measurements of soil CO_2 efflux, volumetric water content, and soil matric potential.

Materials and Methods

Site selection

A replicated study was conducted from 1 June to 11 August 2023 in a tallgrass prairie (39.10220° N, 96.60100° W, 325 m a.s.l.) dominated by Bromegrass (*Bromus inermis* Leyss, *Bromus japonicus* Thunb., *Bromus tectorum* L.) vegetation (Towne, 2002) located at the Konza Prairie Biological Station near Manhattan, KS. The site has a 30-year long-term mean annual precipitation of 909 mm, a mean annual temperature of 12.7 °C (Patrignani et al., 2020), and belongs to the Cfa (Humid subtropical) according to Köppen climate classification (Peel et al., 2007).

Field measurements using instrumented collars

The instrumented collars were constructed using 10-cm diameter polyvinyl chloride (PVC) pipe with a length of 10 cm and a 785 cm^3 volume (Figure 3-1). On one lateral side of the collar, we drilled two holes with a diameter of 3 mm (diameter similar to sensor rods) to insert a volumetric water content sensor (model TEROS 10, Meter Group, Inc.). In this case, the sensor head remained outside of the collars while the sensor rods were inside of the collar, effectively monitoring the water content inside of the collar soil volume. On the opposite lateral side of the collar, we created a notch to tightly pass a soil matric potential

sensor (model TEROS 21, Meter Group, Inc.), which is also equipped with a thermistor that monitored soil temperature. Both openings on the collar wall were centered at 3.5 cm depth. This design allowed us to first insert the collar into undisturbed soil and then insert the sensors with minimal disturbing of the soil within the collar volume. The collars were sharpened on one edge to facilitate insertion into the soil and minimize disturbance and compaction during installation with the help of a wood block and an antivibration hammer. A representative patch in the grassland was selected to install the six instrumented collars, each constituting a replication of the study. Each collar was inserted into the soil until the top edge of the collar was aligned with the soil surface and maintaining a spacing of about 30 cm between the center of adjacent collars.

The TEROS 10 and TEROS 21 sensors were installed by excavating a small volume of soil on the outside of the collars. Right before installing the TEROS 21 sensor, a thick slurry was prepared using native soil to coat the sensor ceramic disc to ensure the soil was in intimate contact with all the surfaces of the ceramic following the manufacturer's recommended installation procedure. In order to obtain a good contact between the TEROS 21 and the surrounding soil, the sensors coated with the slurry were slowly inserted into the collar volume with minimal removal of soil. The installation of the TEROS 10 and TEROS 21 sensors was done immediately following a light rainfall event, when the soil was soft and the sensors were easy to insert. The TEROS 10 and TEROS 21 sensors were connected to a datalogger (model CR300, Campbell Scientific, Inc.) and all raw sensor variables were recorded at hourly intervals and downloaded periodically for inspection and analysis. The area inside and around the collars was maintained free of any vegetation throughout the experiment (Figure 3-2 A). Measurements of volumetric water content and soil matric potential inside the collars were used to create an *in situ* soil water retention curve. To describe the soil water retention curve, we fitted a unimodal van Genuchten model (Eq. 3-1):

$$\frac{\theta-\theta_r}{\theta_s-\theta_r} = [1 + (-\alpha\,\Psi_m)^n]^{-m} \qquad \text{[Eq. 3-1]}$$

where, θ ($cm^3\ cm^{-3}$) is volumetric water content in, θ_r ($cm^3\ cm^{-3}$) is residual volumetric water content, θ_s ($cm^3\ cm^{-3}$) is saturated volumetric water content, Ψ_m (kPa) is soil matric potential, and $\alpha, n,$ and m are fitting parameters, where $m = 1 - 1/n$. In addition, we fitted a Kosugi unimodal model (Eq. 3-2) (Kosugi, 1996):

$$\theta = \frac{1}{2}\,(\theta_s - \theta_r)\,erfc\left(\frac{\ln\left(\frac{x}{hm}\right)}{\sigma\sqrt{2}}\right) + \theta_r \qquad \text{[Eq. 3-2]}$$

where, x (cm) is the median pore radius, hm (cm) is median matric head, σ denotes the standard deviation of ln(x), and *erfc* is the complementary error function. Also, we fitted a Kosugi bimodal model to capture the bimodal pore size distribution (Eq. 3-3, Eq. 3-4, and Eq. 3-5) (Pollacco et al., 2017):

$$\theta_{mac} = \frac{1}{2}\left(\theta_s - \theta_{s_{mac}}\right)erfc\left(\frac{\ln\left(\frac{x}{hm_{mac}}\right)}{\sigma_{mac}\sqrt{2}}\right) + \theta_r \qquad \text{[Eq. 3-3]}$$

$$\theta_{mat} = \frac{1}{2}\left(\theta_{s_{mac}} - \theta_r\right)erfc\left(\frac{\ln\left(\frac{x}{hm}\right)}{\sigma\sqrt{2}}\right) + \theta_r \qquad \text{[Eq. 3-4]}$$

$$\theta = \theta_{mac} + \theta_{mat} \qquad \text{[Eq. 3-5]}$$

where θ_{mac} ($cm^3\ cm^{-3}$) is the volumetric water content for the macropore domain, θ_{s_mac} ($cm^3\ cm^{-3}$) is saturated water content for the macropore domain, hm_{mac} (cm) is the median pore radius of the macropore domain, σ_{mac} is the standard deviation of $\ln(x)$ of the macropore domain, and θ_{mat} ($cm^3\ cm^{-3}$) is the saturated water content of matrix domain.

Soil CO_2 efflux was measured with a portable infrared CO_2 gas analyzer (model EGM-5, PP Systems, Inc.) two to four times per week and at different hours of the day to capture a wide range of soil moisture and soil temperature conditions (Figure 3-2 B). Each soil CO_2 efflux measurement was conducted by placing the portable chamber on the instrumented collar and ensuring good contact with the collar rim to avoid leaks. Each

measurement of soil CO_2 efflux was conducted for 180 seconds. Soil CO_2 efflux was computed as follows:

$$F_{CO2}\ (\mu mol\ m^{-2}\ s^{-1}) = \frac{dC}{dt}\ \frac{P}{1013}\ \frac{273}{273+T_{air}}\ \frac{1}{22.414}\ \frac{V}{A}\ 10^3 \quad \text{[Eq. 3-6]}$$

where, F_{CO2} (µmol m^{-2} s^{-1}) is the soil CO_2 efflux, dC (ppm) is the change in CO_2 concentration, dt (s) is the process time, $\frac{P}{1013}$ is the correction for barometric pressure with P (mbar) measured by the EGM-5, $\frac{1}{22.414}$ (mol m^{-3}) is the standard molar volume of a gas, $\frac{273}{273+T_{air}}$ is the correction for air temperature with T_{air} (°C) input by the user, V (m^3) is the chamber volume, and A (m^2) is soil surface area. When conducting extended measurements during hot days, the portable chamber was insulated using a heat reflecting insulating foam and the gas analyzer was kept under the shade in a portable bag.

A disturbed composite soil sample was collected from the top 10 cm in the surrounding area of the experimental site that was used for phospholipid fatty acid (PLFA) analysis, soil chemical analysis, and particle size analysis. All soil samples were stored in an insulated box during field sampling. Composite soil samples were promptly frozen at -18 °C overnight and subsequently shipped to a professional laboratory (Ward Laboratories, Kearney, NE) for PLFA analysis. Soil chemical analyses included cation exchange capacity (CEC) by the ammonium ion replacement method, organic matter content by the loss on ignition method, total nitrogen and total carbon on a weight percent basis, and pH and bulk electrical conductivity (EC_b) using the saturated paste method (1:1 soil:deionized water) using a calibrated pH and conductivity meter (model PC100, Cole-Parmer, Inc.). Particle size analysis was determined using the hydrometer method (Gavlak et al., 2005). Since soils had a high (i.e., >3.5%) organic matter content, all samples were treated with hydrogen peroxide prior to particle size analysis following the procedure detailed in Gavlak et al. (2005).

Laboratory measurements

At the end of the field study period, the instrumented PVC collars were removed keeping the soil inside the collars intact (Figure 3-3A) and brought to the laboratory to conduct soil matric potential and soil CO_2 efflux measurements under controlled conditions. For each PVC collar we subsampled the soil using a 5 cm height metal ring with a volume of 250 cm^3. The subsampled soil cores were saturated from the bottom up using a 5 mM $CaCl_2$ solution. Saturated soil samples were mounted on the Hyprop system (model Hyprop 2, Meter Group, Inc.) which is an automated hydraulic property analyzer that consists of two precision mini-tensiometers that generate the wet-end (i.e., 0 to -80 kPa) of the soil water retention curve based on the Wind-Schindler's evaporation method (Schindler & Müller, 2006). Throughout the run, soil matric potentials were continuously recorded by the associated Hyprop software (Figure 3-3B). The mass of each Hyprop sensor head with the mounted soil core was recorded between two and four times per day. The average matric potential of each soil sample was computed using the average of both precision mini-tensiometers. Hyprop measurements were terminated and dismounted once both tensiometers cavitated. Then, the soil water potential of four soil samples from each ring was measured using a dew point water potential meter (model WP4C, Meter Group, Inc.) to measure the dry end (i.e., -1,000 to -10,000 kPa) of the soil water retention curve. The WP4C works based on the chilled mirror dew point technique and is often used to extend the typical range of the tensiometers-based Hyprop system. All the samples were oven-dried at 105 °C for 48 hours to determine the corresponding volumetric water content. Bulk density was estimated by dividing the entire mass of oven-dry soil of each ring by the ring volume.

Soil CO_2 efflux was measured with the same portable infrared CO_2 gas analyzer (model EGM-5, PP Systems, Inc.) simultaneously during measurements of soil matric potential with the Hyprop system. Ambient conditions in the laboratory remained constant

with air temperature of 21 ± 1 °C, relative humidity of 55%, and CO_2 concentration of 440 ppm. Soil CO_2 efflux measurements were conducted multiple times per day from saturation conditions and until both of the following two conditions were met: 1) both tensiometers cavitated and 2) EGM-5 CO_2 gas analyzer reading became below 10 ppm, with an approximate difference in CO_2 concentration between two consecutive readings approaching zero. Each measurement of soil CO_2 efflux spanned 180 seconds. A custom 3D-printed plastic sleeve was used to couple the chamber of the portable infrared CO_2 gas analyzer with the samples of the Hyprop system (Figure 3-4). Soil CO_2 efflux was not measured in the dry end of the SWRC measured with the dew point water potential meter since the technique requires the use of small and disturbed soil samples and soil CO_2 efflux readings were usually negligible compared to the observations of field experiment near termination of the Hyprop system.

Statistical analyses

The effect of soil matric potential, volumetric water content, and soil temperature on heterotrophic soil respiration was evaluated using univariate and multivariate linear regression analysis conducted with the *statsmodels* (Seabold & Perktold, 2010) library in the Python programming language. To describe and study the combined effect of soil moisture and soil temperature on soil respiration we implemented a multivariate linear model similar to that of Martin & Bolstad (2005):

$$ln(R_h) = b_0 + b_1 T_{soil} + b_2 {T_{soil}}^2 + b_3 log_{10}(\Psi_m) + b_2 log_{10}(\Psi_m)^2 + b_5 T_{soil} log_{10}(\Psi_m) \quad \text{[Eq. 3-7]}$$

$$ln(R_h) = b_0 + b_1 T_{soil} + b_2 {T_{soil}}^2 + b_3 WFP + b_2 WFP^2 + b_5 T_{soil} WFP \quad \text{[Eq. 3-8]}$$

where R_h (µmol m^{-2} s^{-1}) is the heterotrophic soil respiration, T_{soil} (°C) is the soil temperature at 3.5 cm depth (i.e., center of the collar), Ψ_m (kPa) is the soil matric potential at 3.5 cm depth, and WFP is the water-filled porosity.

Results and Discussion

Field environmental conditions and biophysical properties

During the 72 days of the field study period we collected a total of 48 soil respiration measurements encompassing a wide range of soil temperature and soil moisture conditions. Soil temperature ranged between 15 and 49 °C, soil matric potential ranged from near-saturated conditions (-0.1 kPa) to air-dry conditions (-5,850 kPa), and volumetric soil water content ranged between 0.09 and 0.47 cm^3 cm^{-3} throughout the duration of the experiment (Figure 3-5). The median value for soil matric potential, soil temperature, and volumetric water content were -93 kPa, 27 °C, and 0.31 cm^3 cm^{-3}, respectively. During the study period, there were a total of 19 rainfall events, ranging from 0.25 mm to 44 mm, totaling 201 mm which accounted for 22% of the 30-year long-term mean annual precipitation for this location.

Based on the composite soil samples, the soil of the site had a neutral pH level with a value of 7.3, an EC_b = 314 µS cm^{-1}, CEC = 22.3 meq per 100 g, total nitrogen = 0.30%, and total carbon = 3.42%. As expected, the soil in this grassland had a high organic matter content for soils of this region with a value of 5.9%, suggesting the potential for elevated heterotrophic soil respiration values. The PLFA analysis revealed that the soil microbial community was primarily composed of bacteria (Table 3-1). Microbial community composition and structure are affected by plant species, and the quality and quantity of carbon substrate. Generally, high bacterial populations could be observed in more labile carbon abundant environments. A study conducted on assessing shifts in microbial

community structure in a range of grasslands found that the Gram (-) bacteria population was higher in improved grasslands whereas, fungal and actinomycete populations were higher in unimproved and semi-improved grasslands. The study also concluded that plant species composition was an important factor determining microbial community structure in grasslands (Grayston et al., 2004). Also, the researchers observed a significantly lower bacterial: fungi ratio in semi-improved and unimproved grasslands which were consistent with several other studies (Bardgett et al., 1993, 1998; Grayston et al., 2001).

In situ and laboratory-determined soil water retention curves

Timeseries of *in situ* volumetric water content and soil matric potential were consistent across the six instrumented collars, with average matric potential values differing by no more than 32%, average volumetric water content values differing by <0.04 cm^3 cm^{-3}, and average temperature values differing by <1.5 °C among all collars. Interestingly, the resulting *in situ* SWRC exhibited a bimodal pore size distribution, revealing possible macropores as a result of soil aggregation and faunal activity. As a result, the typical van Genuchten and Kosugi unimodal models, that represent the fine pore matrix of the soil, did not adequately fit our field observations at near-saturation conditions. To circumvent this limitation, a bimodal Kosugi model (Pollacco et al., 2017) was implemented to capture the macropore-matrix pore dynamics (Figure 3-6 A, Table 3-2). The rapid and substantial changes in soil moisture at low tensions revealed the complexity of well-structured prairie soils. Similar findings have been observed in well-aggregated agricultural soils in New Zealand that were also characterized by macropore and matrix pore domains that were captured in soil moisture retention curves (Pollacco et al., 2017).

All six subsampled collars had a bulk density between 1.17 and 1.32 g cm^{-3} with a mean bulk density of 1.21 (SD = 0.07) g cm^{-3}. Saturated volumetric water content of the

subsampled collars ranged between 0.49 and 0.53 cm^3 cm^{-3} with a mean value of 0.51 (SD = 0.02) cm^3 cm^{-3}. The *in situ* SWRC revealed a bimodal pore size distribution, likely arising from the presence of macropores formed through soil aggregation, faunal activities, and root interactions. These macropores likely emptied at low tensions, substantially changing the volumetric water content of the soil volume. Another option is that perhaps macropores and cracks were never filled with water, even during copious rainfall events. Since our observations were made at hourly time intervals, some of these dynamics occurring at the second or minute time scales were not captured with sufficient level of temporal detail to examine the process in more detail. In contrast, the laboratory determined SWRC did not exhibit a bimodal pore size distribution, which was possibly caused by the small sensing volume of the tensiometers and the lack of free drainage of the saturated samples mounted in the Hyprop system, which affect the wet end of the soil water retention curve. Our findings show the importance of *in situ* SWRC determination in characterizing field soil moisture conditions, providing valuable insights into the matric potential–soil respiration relationship.

Typically, SWRC are determined in a controlled laboratory conditions and the resulting SWRCs are treated as a time-invariant soil property. The proposed instrumented collars with collocated sensors of volumetric water content and soil matric potential offers a new possibility for measuring SWRC during different drydown events to better capture water retention characteristics of the soil (Figure 3-7). Differences between *in situ* SWRC could be attributed to changes in the pore space due to the re-arrangement of particles and aggregates caused by water transport, faunal activity, and shrinking and swelling due to wetting and drying cycles that can affect the water retention characteristics of the soil. Furthermore, some of these *in situ* measurements could also be used for capturing daily and seasonal dynamics in soil respiration modeling studies (Johnson et al., 2013; Pečan et al., 2023).

Relationship of heterotrophic respiration with environmental factors

In situ observations of soil CO_2 efflux showed a significant (P=0.000) positive linear (r = 0.65) relationship with water-filled porosity (Figure 3-8 A) and a significant (P=0.000) slightly weaker negative linear (r = -0.64) relationship with soil matric potential (Figure 3-8 B). Part of the reason for the somewhat low correlation between soil CO_2 efflux and both soil moisture indicators may be associated to the confounding effect of soil temperature. In general, the highest microbial activity in terms of soil CO_2 efflux was observed near water-filled porosity in the range of 0.8 to 0.9 and at soil temperatures between 28 and 33 °C (Figure 3-9). The maximum recorded soil CO_2 efflux value of 7.10 µmol m^{-2} s^{-1} was observed around -30 kPa soil matric potential on June 15th 2023 at 35 °C soil temperature and 0.36 volumetric water content.

The mean CO_2 efflux from the experimental site during the study period was 4.40 µmol m^{-2} s^{-1} which is about 1 µmol m^{-2} s^{-1} higher than the observations of soil CO_2 efflux studies within the same as well as in nearby prairie ecosystems. For example, a study conducted on the response of soil respiration to clipping and grazing in a tallgrass prairie in northeastern Kansas reported an average soil CO_2 efflux of 3.56 µmol m^{-2} s^{-1} in no-clipping pastures (Bremer et al., 1998), while a study conducted in tallgrass prairie in the Konza Prairie Biological Station during the summer of 1987 and 1988 has recorded mean soil respirations of 3.08 (SD = 1.16) µmol m^{-2} s^{-1} in 1987 and 2.55 (SD = 1.30) µmol m^{-2} s^{-1} in 1988 (Franzluebbers et al., 2002). Another study conducted on soil respiration in a tallgrass prairie in Missouri reported a 2.84 µmol m^{-2} s^{-1} average soil CO_2 efflux in the summer period (Kucera & Kirkham, 1971). These elevated mean soil CO_2 efflux observations in the present study could be attributed to two possible reasons including temporal and spatial variability which will cause differences in soil temperature, soil moisture, and substrate availability. Also, there could be an effect of the method used to measure soil CO_2 efflux. For example,

soil warming caused by soil respiration chambers can indirectly lead to increased soil respiration due to the increased availability of carbon substrates (Shaver et al., 2000). Normalized CO_2 efflux values for both laboratory and field measurements revealed that the maximum CO_2 efflux occurred within the range of 0 to -100 kPa and around 0.8 water-filled porosity (Figure 3-10).

Conclusions

In situ measurements of soil matric potential and volumetric water content with respiration collars unveiled possible hysteric effects and characteristic macropore-matrix soil moisture dynamics likely caused by well-aggregated soil that were characterized by a bimodal soil moisture retention curve, which are not typically observed in laboratory setup. Our findings highlight that future research aimed at better understanding the relationship between heterotrophic soil respiration and soil water potential would benefit from *in situ* measurements, particularly in well-aggregated soils and soil moisture conditions near or above 0.8 water-filled porosity. This finding is relevant as many of the soil property databases available in the scientific literature are based on laboratory determination, which may hinder accurate predictions of soil respiration in land surface models. Water-filled porosity showed a stronger correlation with heterotrophic soil CO_2 efflux across a wide spectrum of soil temperature than soil matric potential. Therefore, we reject our initial hypothesis that soil matric potential has an advantage over simpler volumetric soil moisture indicators. Looking forward, future research that combines instrumented collars with automated soil CO_2 chambers holds promise for gaining deeper insights into temporal and spatial dynamics of heterotrophic soil respiration in response to varying soil temperature and moisture conditions, spanning from air-dry to near saturation soil moisture conditions.

References

Aerts, R., & Heil, G. W. (Eds.). (2013). Heathlands: Patterns and processes in a changing environment (Vol. 20). Springer Science & Business Media.

Andraski, B. J., & Scanlon, B. R. (2018). 3.2.3 Thermocouple psychrometry. In J. H. Dane & G. Clarke Topp (Eds.), *SSSA Book Series* (pp. 609–642). Soil Science Society of America. https://doi.org/10.2136/sssabookser5.4.c22

Bardgett, R. D., Frankland, J. C., & Whittaker, J. B. (1993). The effects of agricultural management on the soil biota of some upland grasslands. *Agriculture, Ecosystems & Environment*, *45*(1–2), 25–45. https://doi.org/10.1016/0167-8809(93)90057-V

Bardgett, R. D., Wardle, D. A., & Yeates, G. W. (1998). Linking above-ground and below-ground interactions: How plant responses to foliar herbivory influence soil organisms. *Soil Biology and Biochemistry*, *30*(14), 1867–1878. https://doi.org/10.1016/S0038-0717(98)00069-8

Bauer, J., Weihermüller, L., Huisman, J. A., Herbst, M., Graf, A., Séquaris, J. M., & Vereecken, H. (2012). Inverse determination of heterotrophic soil respiration response to temperature and water content under field conditions. *Biogeochemistry*, *108*(1–3), 119–134. https://doi.org/10.1007/s10533-011-9583-1

Bradford, M. A., Davies, C. A., Frey, S. D., Maddox, T. R., Melillo, J. M., Mohan, J. E., Reynolds, J. F., Treseder, K. K., & Wallenstein, M. D. (2008). Thermal adaptation of soil microbial respiration to elevated temperature. *Ecology Letters*, *11*(12), 1316–1327. https://doi.org/10.1111/j.1461-0248.2008.01251.x

Bremer, D. J., Ham, J. M., Owensby, C. E., & Knapp, A. K. (1998). Responses of soil respiration to clipping and grazing in a tallgrass prairie. *Journal of Environmental Quality*, *27*(6), 1539–1548. https://doi.org/10.2134/jeq1998.00472425002700060034x

Chandra, L. R., Gupta, S., Pande, V., & Singh, N. (2016). Impact of forest vegetation on soil characteristics: A correlation between soil biological and physico-chemical properties. *3 Biotech*, *6*(2), 188. https://doi.org/10.1007/s13205-016-0510-y

Christensen, T. R., Jonasson, S., Callaghan, T. V., & Havström, M. (1999). On the potential CO_2 release from tundra soils in a changing climate. *Applied Soil Ecology*, *11*(2–3), 127–134. https://doi.org/10.1016/S0929-1393(98)00146-2

Ciocca, F., Lunati, I., & Parlange, M. B. (2014). Effects of the water retention curve on evaporation from arid soils. *Geophysical Research Letters*, *41*(9), 3110–3116. https://doi.org/10.1002/2014GL059827

Conant, R. T., Dalla-Betta, P., Klopatek, C. C., & Klopatek, J. M. (2004). Controls on soil respiration in semiarid soils. *Soil Biology and Biochemistry*, *36*(6), 945–951. https://doi.org/10.1016/j.soilbio.2004.02.013

Cook, F. J., & Orchard, V. A. (2008). Relationships between soil respiration and soil moisture. *Soil Biology and Biochemistry*, *40*(5), 1013–1018. https://doi.org/10.1016/j.soilbio.2007.12.012

Cox, P. M., Betts, R. A., Jones, C. D., Spall, S. A., & Totterdell, I. J. (2000). Acceleration of global warming due to carbon-cycle feedbacks in a coupled climate model. *Nature*, *408*(6809), 184–187. https://doi.org/10.1038/35041539

Curiel Yuste, J., Baldocchi, D. D., Gershenson, A., Goldstein, A., Misson, L., & Wong, S. (2007). Microbial soil respiration and its dependency on carbon inputs, soil temperature and moisture. *Global Change Biology*, *13*(9), 2018–2035. https://doi.org/10.1111/j.1365-2486.2007.01415.x

Davidson, E. A., & Janssens, I. A. (2006a). Temperature sensitivity of soil carbon decomposition and feedbacks to climate change. *Nature*, *440*(7081), 165–173. https://doi.org/10.1038/nature04514

Davidson, E. A., & Janssens, I. A. (2006b). Temperature sensitivity of soil carbon decomposition and feedbacks to climate change. *Nature*, *440*(7081), 165–173. https://doi.org/10.1038/nature04514

Davidson, EriC. A., Belk, E., & Boone, R. D. (1998). Soil water content and temperature as independent or confounded factors controlling soil respiration in a temperate mixed hardwood forest. *Global Change Biology*, *4*(2), 217–227. https://doi.org/10.1046/j.1365-2486.1998.00128.x

Eliasson, P. E., McMurtrie, R. E., Pepper, D. A., Strömgren, M., Linder, S., & Ågren, G. I. (2005). The response of heterotrophic CO_2 flux to soil warming. *Global Change Biology*, *11*(1), 167–181. https://doi.org/10.1111/j.1365-2486.2004.00878.x

Fang, C., & Moncrieff, J. B. (2001). The dependence of soil CO_2 efflux on temperature. *Soil Biology and Biochemistry*, *33*(2), 155–165. https://doi.org/10.1016/S0038-0717(00)00125-5

Fang, H., Cheng, S., Wang, Y., Yu, G., Xu, M., Dang, X., Li, L., & Wang, L. (2014). Changes in soil heterotrophic respiration, carbon availability, and microbial function in seven forests along a climate gradient. *Ecological Research*, *29*(6), 1077–1086. https://doi.org/10.1007/s11284-014-1194-6

Fischer, T. (2009). Substantial rewetting phenomena on soil respiration can be observed at low water availability. *Soil Biology and Biochemistry*, *41*(7), 1577–1579. https://doi.org/10.1016/j.soilbio.2009.04.009

Franzluebbers, K., Franzluebbers, A. J., & Jawson, M. D. (2002). Environmental controls on soil and whole-ecosystem respiration from a tallgrass prairie. *Soil Science Society of America Journal*, *66*(1), 254–262. https://doi.org/10.2136/sssaj2002.2540

Friend, A. D., Arneth, A., Kiang, N. Y., Lomas, M., Ogée, J., Rödenbeck, C., Running, S. W., Santaren, J.-D., Sitch, S., Viovy, N., Ian Woodward, F., & Zaehle, S. (2007).

FLUXNET and modelling the global carbon cycle. *Global Change Biology*, *13*(3), 610–633. https://doi.org/10.1111/j.1365-2486.2006.01223.x

G. Selassie, Y., & Ayanna, G. (2013). Effects of different land use systems on selected physico-chemical properties of soils in northwestern Ethiopia. *Journal of Agricultural Science*, *5*(4), p112. https://doi.org/10.5539/jas.v5n4p112

Grayston, S. J., Campbell, C. D., Bardgett, R. D., Mawdsley, J. L., Clegg, C. D., Ritz, K., Griffiths, B. S., Rodwell, J. S., Edwards, S. J., Davies, W. J., Elston, D. J., & Millard, P. (2004). Assessing shifts in microbial community structure across a range of grasslands of differing management intensity using CLPP, PLFA and community DNA techniques. *Applied Soil Ecology*, *25*(1), 63–84. https://doi.org/10.1016/S0929-1393(03)00098-2

Grayston, S. J., Griffith, G. S., Mawdsley, J. L., Campbell, C. D., & Bardgett, R. D. (2001). Accounting for variability in soil microbial communities of temperate upland grassland ecosystems. *Soil Biology and Biochemistry*, *33*(4–5), 533–551. https://doi.org/10.1016/S0038-0717(00)00194-2

Guimberteau, M., Zhu, D., Maignan, F., Huang, Y., Yue, C., Dantec-Nédélec, S., Ottlé, C., Jornet-Puig, A., Bastos, A., Laurent, P., Goll, D., Bowring, S., Chang, J., Guenet, B., Tifafi, M., Peng, S., Krinner, G., Ducharne, A., Wang, F., … Ciais, P. (2018). ORCHIDEE-MICT (v8.4.1), a land surface model for the high latitudes: Model description and validation. *Geoscientific Model Development*, *11*(1), 121–163. https://doi.org/10.5194/gmd-11-121-2018

Gulledge, J., & Schimel, J. P. (1998). Moisture control over atmospheric CH_4 consumption and CO_2 production in diverse Alaskan soils. *Soil Biology and Biochemistry*, *30*(8–9), 1127–1132. https://doi.org/10.1016/S0038-0717(97)00209-5

Hamdi, S., Chevallier, T., Ben Aïssa, N., Ben Hammouda, M., Gallali, T., Chotte, J.-L., & Bernoux, M. (2011). Short-term temperature dependence of heterotrophic soil respiration after one-month of pre-incubation at different temperatures. *Soil Biology and Biochemistry*, *43*(9), 1752–1758. https://doi.org/10.1016/j.soilbio.2010.05.025

Hartley, I. P., Heinemeyer, A., & Ineson, P. (2007). Effects of three years of soil warming and shading on the rate of soil respiration: Substrate availability and not thermal acclimation mediates observed response. *Global Change Biology*, *13*(8), 1761–1770. https://doi.org/10.1111/j.1365-2486.2007.01373.x

Hartley, I. P., Hopkins, D. W., Garnett, M. H., Sommerkorn, M., & Wookey, P. A. (2008). Soil microbial respiration in arctic soil does not acclimate to temperature. *Ecology Letters*, *11*(10), 1092–1100. https://doi.org/10.1111/j.1461-0248.2008.01223.x

Hobbie, S. E., Schimel, J. P., Trumbore, S. E., & Randerson, J. R. (2000). Controls over carbon storage and turnover in high-latitude soils. *Global Change Biology*, *6*(S1), 196–210. https://doi.org/10.1046/j.1365-2486.2000.06021.x

Hui, D., & Luo, Y. (2004). Evaluation of soil CO_2 production and transport in Duke Forest using a process-based modeling approach. *Global Biogeochemical Cycles*, *18*(4), 2004GB002297. https://doi.org/10.1029/2004GB002297

Hursh, A., Ballantyne, A., Cooper, L., Maneta, M., Kimball, J., & Watts, J. (2017). The sensitivity of soil respiration to soil temperature, moisture, and carbon supply at the global scale. *Global Change Biology*, *23*(5), 2090–2103. https://doi.org/10.1111/gcb.13489

Ilstedt, U., Nordgren, A., & Malmer, A. (2000). Optimum soil water for soil respiration before and after amendment with glucose in humid tropical acrisols and a boreal mor layer. *Soil Biology and Biochemistry*, *32*(11–12), 1591–1599. https://doi.org/10.1016/S0038-0717(00)00073-0

Jayarathne, J. R. R. N., Chamindu Deepagoda, T. K. K., Clough, T. J., Thomas, S., Elberling, B., & Smits, K. M. (2021). Effect of aggregate size distribution on soil moisture, soil-gas diffusivity, and N_2O emissions from a pasture soil. *Geoderma*, *383*, 114737. https://doi.org/10.1016/j.geoderma.2020.114737

Johnson, D. D., & Guenzi, W. D. (1963). Influence of salts on ammonium oxidation and carbon dioxide evolution from soil. *Soil Science Society of America Journal*, *27*(6), 663–666. https://doi.org/10.2136/sssaj1963.03615995002700060028x

Johnson, M. S., Couto, E. G., Pinto Jr, O. B., Milesi, J., Santos Amorim, R. S., Messias, I. A. M., & Biudes, M. S. (2013). Soil CO_2 dynamics in a tree island soil of the Pantanal: The role of soil water potential. *PLoS ONE*, *8*(6), e64874. https://doi.org/10.1371/journal.pone.0064874

Keesstra, S., Geissen, V., Mosse, K., Piiranen, S., Scudiero, E., Leistra, M., & Van Schaik, L. (2012). Soil as a filter for groundwater quality. *Current Opinion in Environmental Sustainability*, *4*(5), 507–516. https://doi.org/10.1016/j.cosust.2012.10.007

Kekane, S. (2015). A review on physico-chemical properties of soil. *International Journal of Chemical Studies*, *3*(4), 29–32.

Kirschbaum, M. U. F. (2004). Soil respiration under prolonged soil warming: Are rate reductions caused by acclimation or substrate loss? *Global Change Biology*, *10*(11), 1870–1877. https://doi.org/10.1111/j.1365-2486.2004.00852.x

Klemedtsson, L., Von Arnold, K., Weslien, P., & Gundersen, P. (2005). Soil C:N ratio as a scalar parameter to predict nitrous oxide emissions. *Global Change Biology*, *11*(7), 1142–1147. https://doi.org/10.1111/j.1365-2486.2005.00973.x

Knorr, W., Prentice, I. C., House, J. I., & Holland, E. A. (2005). Long-term sensitivity of soil carbon turnover to warming. *Nature*, *433*(7023), 298–301. https://doi.org/10.1038/nature03226

Kosugi, K. (1996). Lognormal distribution model for unsaturated soil hydraulic properties. *Water Resources Research*, *32*(9), 2697–2703. https://doi.org/10.1029/96WR01776

Kucera, C. L., & Kirkham, D. R. (1971). Soil respiration studies in tallgrass prairie in Missouri. *Ecology*, *52*(5), 912–915. https://doi.org/10.2307/1936043

Lellei-Kovács, E., Kovács-Láng, E., Botta-Dukát, Z., Kalapos, T., Emmett, B., & Beier, C. (2011). Thresholds and interactive effects of soil moisture on the temperature response of soil respiration. *European Journal of Soil Biology*, *47*(4), 247–255. https://doi.org/10.1016/j.ejsobi.2011.05.004

Lessard, R., Rochette, P., Topp, E., Pattey, E., Desjardins, R. L., & Beaumont, G. (1994). Methane and carbon dioxide fluxes from poorly drained adjacent cultivated and forest sites. *Canadian Journal of Soil Science*, *74*(2), 139–146. https://doi.org/10.4141/cjss94-021

Li, X., Guo, D., Zhang, C., Niu, D., Fu, H., & Wan, C. (2018). Contribution of root respiration to total soil respiration in a semi-arid grassland on the Loess Plateau, China. *Science of The Total Environment*, *627*, 1209–1217. https://doi.org/10.1016/j.scitotenv.2018.01.313

Li, Y., Xu, M., & Zou, X. (2006). Heterotrophic soil respiration in relation to environmental factors and microbial biomass in two wet tropical forests. *Plant and Soil*, *281*(1–2), 193–201. https://doi.org/10.1007/s11104-005-4249-1

Linn, D. M., & Doran, J. W. (1984). Effect of water-filled pore space on carbon dioxide and nitrous oxide production in tilled and non-tilled soils. *Soil Science Society of America Journal*, *48*(6), 1267–1272. https://doi.org/10.2136/sssaj1984.03615995004800060013x

Lloyd, J., & Taylor, J. A. (1994). On the temperature dependence of soil respiration. *Functional Ecology*, *8*(3), 315. https://doi.org/10.2307/2389824

Luo, Y., Wan, S., Hui, D., & Wallace, L. L. (2001). Acclimatization of soil respiration to warming in a tall grass prairie. *Nature*, *413*(6856), 622–625. https://doi.org/10.1038/35098065

Manzoni, S., Schimel, J. P., & Porporato, A. (2012). Responses of soil microbial communities to water stress: Results from a meta-analysis. *Ecology*, *93*(4), 930–938. https://doi.org/10.1890/11-0026.1

Martin, J. G., & Bolstad, P. V. (2005). Annual soil respiration in broadleaf forests of northern Wisconsin: Influence of moisture and site biological, chemical, and physical characteristics. *Biogeochemistry*, *73*(1), 149–182. https://doi.org/10.1007/s10533-004-5166-8

Meyer, N., Welp, G., & Amelung, W. (2019). Effect of sieving and sample storage on soil respiration and its temperature sensitivity (Q10) in mineral soils from Germany. *Biology and Fertility of Soils*, *55*(8), 825–832. https://doi.org/10.1007/s00374-019-01374-7

Moyano, F. E., Manzoni, S., & Chenu, C. (2013). Responses of soil heterotrophic respiration to moisture availability: An exploration of processes and models. *Soil Biology and Biochemistry*, *59*, 72–85. https://doi.org/10.1016/j.soilbio.2013.01.002

Mu, Z., Huang, A., Ni, J., & Xie, D. (2014). Linking annual N_2O emission in organic soils to mineral nitrogen input as estimated by heterotrophic respiration and soil C/N ratio. *PLoS ONE*, *9*(5), e96572. https://doi.org/10.1371/journal.pone.0096572

Nakas, J. P., & Klein, D. A. (1979). Decomposition of microbial cell components in a semi-arid grassland soil. *Applied and Environmental Microbiology*, *38*(3), 454–460. https://doi.org/10.1128/aem.38.3.454-460.1979

Neff, J. C., & Hooper, D. U. (2002). Vegetation and climate controls on potential CO_2, DOC and DON production in northern latitude soils: Climate and vegetation controls over

soil organic matter dynamics. *Global Change Biology*, *8*(9), 872–884. https://doi.org/10.1046/j.1365-2486.2002.00517.x

Nielsen, D. R., Th. Van Genuchten, M., & Biggar, J. W. (1986). Water flow and solute transport processes in the unsaturated zone. *Water Resources Research*, *22*(9S). https://doi.org/10.1029/WR022i09Sp0089S

Novick, K. A., Ficklin, D. L., Baldocchi, D., Davis, K. J., Ghezzehei, T. A., Konings, A. G., MacBean, N., Raoult, N., Scott, R. L., Shi, Y., Sulman, B. N., & Wood, J. D. (2022). Confronting the water potential information gap. *Nature Geoscience*, *15*(3), 158–164. https://doi.org/10.1038/s41561-022-00909-2

Orchard, V. A., & Cook, F. J. (1983). Relationship between soil respiration and soil moisture. *Soil Biology and Biochemistry*, *15*(4), 447–453. https://doi.org/10.1016/0038-0717(83)90010-X

Parker, N., Kluitenberg, G. J., Redmond, C., & Patrignani, A. (2022). A database of soil physical properties for the Kansas Mesonet. *Soil Science Society of America Journal*, *86*(6), 1495–1508. https://doi.org/10.1002/saj2.20465

Patrignani, A., Knapp, M., Redmond, C., & Santos, E. (2020). Technical overview of the Kansas Mesonet. *Journal of Atmospheric and Oceanic Technology*, *37*(12), 2167-2183.

Pečan, U., Pintar, M., Mihelič, R., & Kastelec, D. (2023). Variability of in situ soil water retention curves under different tillage systems and growing seasons. *Soil and Tillage Research*, *233*, 105779. https://doi.org/10.1016/j.still.2023.105779

Peel, M. C., Finlayson, B. L., & McMahon, T. A. (2007). Updated world map of the Köppen-Geiger climate classification. *Hydrology and Earth System Sciences*, *11*(5), 1633–1644. https://doi.org/10.5194/hess-11-1633-2007

Pollacco, J. A. P., Webb, T., McNeill, S., Hu, W., Carrick, S., Hewitt, A., & Lilburne, L. (2017). Saturated hydraulic conductivity model computed from bimodal water retention curves for a range of New Zealand soils. *Hydrology and Earth System Sciences*, *21*(6), 2725–2737. https://doi.org/10.5194/hess-21-2725-2017

Priha, O., Grayston, S. J., Hiukka, R., Pennanen, T., & Smolander, A. (2001). Microbial community structure and characteristics of the organic matter in soils under *Pinus sylvestris*, *Picea abies* and *Betula pendula* at two forest sites. *Biology and Fertility of Soils*, *33*(1), 17–24. https://doi.org/10.1007/s003740000281

Pumpanen, J., Ilvesniemi, H., & Hari, P. (2003). A process-based model for predicting soil carbon dioxide efflux and concentration. *Soil Science Society of America Journal*, *67*(2), 402–413. https://doi.org/10.2136/sssaj2003.4020

Raich, J. W., & Schlesinger, W. H. (1992). The global carbon dioxide flux in soil respiration and its relationship to vegetation and climate. *Tellus B*, *44*(2), 81–99. https://doi.org/10.1034/j.1600-0889.1992.t01-1-00001.x

Raich, J. W., & Tufekciogul, A. (2000a). Vegetation and soil respiration: Correlations and controls. *Biogeochemistry*, *48*(1), 71–90. https://doi.org/10.1023/A:1006112000616

Reichstein, M., Rey, A., Freibauer, A., Tenhunen, J., Valentini, R., Banza, J., Casals, P., Cheng, Y., Grünzweig, J. M., Irvine, J., Joffre, R., Law, B. E., Loustau, D., Miglietta, F., Oechel, W., Ourcival, J., Pereira, J. S., Peressotti, A., Ponti, F., … Yakir, D. (2003). Modeling temporal and large-scale spatial variability of soil respiration from soil water availability, temperature and vegetation productivity indices. *Global Biogeochemical Cycles*, *17*(4), 2003GB002035. https://doi.org/10.1029/2003GB002035

Reichstein, M., Subke, J., Angeli, A. C., & Tenhunen, J. D. (2005). Does the temperature sensitivity of decomposition of soil organic matter depend upon water content, soil

horizon, or incubation time? *Global Change Biology*, *11*(10), 1754–1767. https://doi.org/10.1111/j.1365-2486.2005.001010.x

Rodeghiero, M., & Cescatti, A. (2005). Main determinants of forest soil respiration along an elevation/temperature gradient in the Italian Alps. *Global Change Biology*, *11*(7), 1024–1041. https://doi.org/10.1111/j.1365-2486.2005.00963.x

Schimel, J. P., Gulledge, J. M., Clein-Curley, J. S., Lindstrom, J. E., & Braddock, J. F. (1999). Moisture effects on microbial activity and community structure in decomposing birch litter in the Alaskan taiga. *Soil Biology and Biochemistry*, *31*(6), 831–838. https://doi.org/10.1016/S0038-0717(98)00182-5

Schindlbacher, A., Zechmeister-Boltenstern, S., & Jandl, R. (2009). Carbon losses due to soil warming: Do autotrophic and heterotrophic soil respiration respond equally? *Global Change Biology*, *15*(4), 901–913. https://doi.org/10.1111/j.1365-2486.2008.01757.x

Schindler, U., & Müller, L. (2006). Simplifying the evaporation method for quantifying soil hydraulic properties. *Journal of Plant Nutrition and Soil Science*, *169*(5), 623–629. https://doi.org/10.1002/jpln.200521895

Schnürer, J., Clarholm, M., Boström, S., & Rosswall, T. (1986). Effects of moisture on soil microorganisms and nematodes: A field experiment. *Microbial Ecology*, *12*(2), 217–230. https://doi.org/10.1007/BF02011206

Seabold, S., & Perktold, J. (2010, June). Statsmodels: Econometric and statistical modeling with python. In *Proceedings of the 9th Python in Science Conference* (Vol. 57, No. 61, pp. 10-25080).

Shaver, G. R., Canadell, J., Chapin, F. S., Gurevitch, J., Harte, J., Henry, G., Ineson, P., Jonasson, S., Melillo, J., Pitelka, L., & Rustad, L. (2000). Global warming and terrestrial ecosystems: A conceptual framework for analysis. *BioScience*, *50*(10), 871. https://doi.org/10.1641/0006-3568(2000)050[0871:GWATEA]2.0.CO;2

Singh, B. R., Agarwal, A. S., & Kanehiro, Y. (1969). Effect of chloride salts on ammonium nitrogen release in two Hawaiian soils. *Soil Science Society of America Journal*, *33*(4), 557–560. https://doi.org/10.2136/sssaj1969.03615995003300040021x

Stocker, T. (Ed.). (2014). *Climate change 2013: The physical science basis: Working Group I contribution to the Fifth assessment report of the Intergovernmental Panel on Climate Change*. Cambridge University Press.

Striegl, R. G., & Wickland, K. P. (1998). Effects of a clear-cut harvest on soil respiration in a jack pine—Lichen woodland. *Canadian Journal of Forest Research*, *28*(4), 534–539. https://doi.org/10.1139/x98-023

Torbert, H. A., & Wood, C. W. (1992). Effects of soil compaction and water-filled pore space on soil microbial activity and N losses. *Communications in Soil Science and Plant Analysis*, *23*(11–12), 1321–1331. https://doi.org/10.1080/00103629209368668

Towne, E. G. (2002). Vascular plants of Konza prairie biological station: An annotated checklist of species in a Kansas tallgrass prairie. *SIDA, Contributions to Botany*, *20*(1), 269–294.

Tufekcioglu, A., Raich, J. W., Isenhart, T. M., & Schultz, R. C. (2001). Soil respiration within riparian buffers and adjacent crop fields. *Plant and Soil*, *229*(1), 117–124. https://doi.org/10.1023/A:1004818422908

Van Genuchten, M. Th. (1980). A closed-form equation for predicting the hydraulic conductivity of unsaturated soils. *Soil Science Society of America Journal*, *44*(5), 892–898. https://doi.org/10.2136/sssaj1980.03615995004400050002x

Whalley, W. R., Ober, E. S., & Jenkins, M. (2013). Measurement of the matric potential of soil water in the rhizosphere. *Journal of Experimental Botany*, *64*(13), 3951–3963. https://doi.org/10.1093/jxb/ert044

Wickland, K. P., & Neff, J. C. (2008). Decomposition of soil organic matter from boreal black spruce forest: Environmental and chemical controls. *Biogeochemistry*, *87*(1), 29–47. https://doi.org/10.1007/s10533-007-9166-3

Xu, Z., Zhang, T., Wang, S., & Wang, Z. (2020). Soil pH and C/N ratio determines spatial variations in soil microbial communities and enzymatic activities of the agricultural ecosystems in Northeast China: Jilin Province case. *Applied Soil Ecology*, *155*, 103629. https://doi.org/10.1016/j.apsoil.2020.103629

Xue, D., Yao, H.-Y., Ge, D.-Y., & Huang, C.-Y. (2008). Soil microbial community structure in diverse land use systems: A comparative study using Biolog, DGGE, and PLFA analyses. *Pedosphere*, *18*(5), 653–663. https://doi.org/10.1016/S1002-0160(08)60060-0

Yan, Z., Liu, C., Todd-Brown, K. E., Liu, Y., Bond-Lamberty, B., & Bailey, V. L. (2016). Pore-scale investigation on the response of heterotrophic respiration to moisture conditions in heterogeneous soils. *Biogeochemistry*, *131*(1–2), 121–134. https://doi.org/10.1007/s10533-016-0270-0

Zhang, W., Parker, K. M., Luo, Y., Wan, S., Wallace, L. L., & Hu, S. (2005). Soil microbial responses to experimental warming and clipping in a tallgrass prairie. *Global Change Biology*, *11*(2), 266–277. https://doi.org/10.1111/j.1365-2486.2005.00902.x

Zhou, W., Hui, D., & Shen, W. (2014). Effects of soil moisture on the temperature sensitivity of soil heterotrophic respiration: A laboratory incubation study. *PLoS ONE*, *9*(3), e92531. https://doi.org/10.1371/journal.pone.0092531

Zogg, G. P., Zak, D. R., Ringelberg, D. B., White, D. C., MacDonald, N. W., & Pregitzer, K. S. (1997). Compositional and functional shifts in microbial communities due to soil warming. *Soil Science Society of America Journal*, *61*(2), 475–481. https://doi.org/10.2136/sssaj1997.03615995006100020015x

Table 3-1: Biomass of total bacteria, Gram (+) bacteria, Gram (-) bacteria, total fungi, and protozoa of each site at sampling by Phospholipid Fatty Acid analysis (PLFA). Numbers within brackets indicate the percentage of each microbial community in total microbial biomass.

Functional group	**Biomass PLFA**
	ng g^{-1} soil (%)
Bacteria	3,296 (47.2)
Gram (+)	1,950 (27.9)
Gram (-)	1,346 (19.3)
Fungi	988 (14.1)
Protozoa	15 (0.2)
Undifferentiated	2,685 (38.5)
Total[†]	6,983 (100)

[†] Total biomass PLFA was computed as the sum of bacteria, fungi, protozoa, and undifferentiated functional groups.

Table 3-2: Model Parameters for Fitted van Genuchten, Kosugi Unimodal, and Kosugi Bimodal for in situ and laboratory-determined soil water retention curves. The parameters represent θ_s for saturated volumetric water content, θ_r for residual volumetric water content, α and n are the fitting parameters for van Genuchten model, and h_m, σ, h_{m-mac}, σ_{mac}, and θ_{s-mac} represent the median matric head, the standard deviation of the natural logarithm of the median pore radius, the median pore radius of the macro pore domain, the standard deviation of the natural logarithm of the median pore radius of the macro pore domain, and the saturated water content for the macro pore domain, respectively for the Kosugi unimodal and bimodal models.

Model	θ_s	θ_r	α	n	h_m	σ	h_{m-mac}	σ_{mac}	θ_{s-mac}
	$cm^3\ cm^{-3}$	$cm^3\ cm^{-3}$	kPa^{-1}	-	cm	-	cm	-	$cm^3\ cm^{-3}$
van Genuchten in situ	0.303	3.55×10^{-16}	0.088	1.26					
van Genuchten lab	0.507	0.025	0.171	1.25					
Kosugi unimodal in situ	0.336	1.46×10^{-2}			0.998	3.50			
Kosugi unimodal lab	0.512	0.118			40.4	2.09			
Kosugi bimodal in situ	0.274	2.61×10^{-2}			0.971	3.18	0.225	0.135	0.176

Table 3-3: Multivariate linear regression analysis for models explaining heterotrophic soil respiration ($\ln(R_h)$) as a function of soil temperature (T_{soil}), water-filled porosity (wfp), and soil matric potential (Ψ_m) variables for statistical analysis results for two models.

Model terms	Coefficient value	Standard error	$P > \|t\|^{\dagger}$
Model 1			
Intercept	4.368	1.836	0.022
T_{soil}	-0.201	0.088	0.027*
wfp	-2.314	2.383	0.337
$T_{soil} : wfp$	0.096	0.042	0.027*
wfp^2	0.512	1.054	0.630
${T_{soil}}^2$	0.003	0.001	0.030*
Model 2			
Intercept	1.805	1.055	0.095
T_{soil}	-0.061	0.068	0.374
$log_{10}\Psi_m$	0.391	0.239	0.109
$T_{soil} : log_{10}\Psi_m$	-0.020	0.008	0.016*
${log_{10}\Psi_m}^2$	-0.005	0.032	0.883
${T_{soil}}^2$	0.002	0.001	0.098

† * means significant differences at $P<0.05$

Table 3-4: Overall model results for multivariate linear regression analysis for two models explaining heterotrophic soil respiration ($\ln(R_h)$) as a function of soil temperature (T_{soil}), water-filled porosity (wfp), and soil matric potential (Ψ_m) variables for statistical analysis.

Independent variables	R^2	Adj. R^2	*F*-statistic	Prob *(F*-statistic)	AIC
T_{soil} and $log_{10}\Psi_m$	0.560	0.507	10.68	1.14×10^{-6}	-4.403
T_{soil} and WFP	0.619	0.574	13.64	6.38×10^{-8}	-11.32

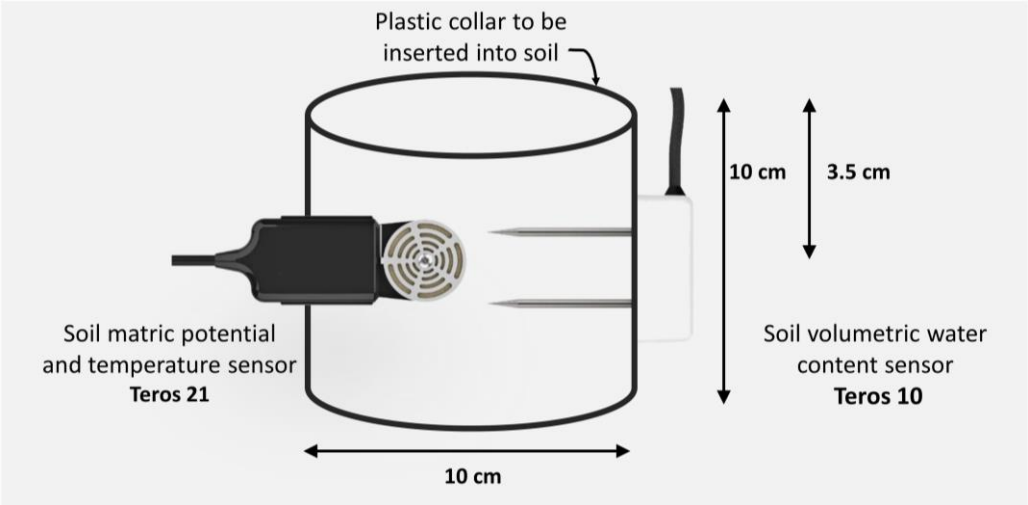

Figure 3-1: Instrumented collar for collocated measurements of heterotrophic soil respiration (model EGM-5, PP Systems), soil matric potential (model TEROS 21, Meter Group, Inc.), soil temperature (model TEROS 21, Meter Group, Inc.), and volumetric water content (model TEROS 10, Meter Group, Inc.).

Figure 3-2: A) An installed instrumented PVC collar with sensors for measuring heterotrophic soil respiration, soil matric potential (model TEROS 21, Meter Group, Inc.), soil temperature (model TEROS 21, Meter Group, Inc.), and volumetric water content (model TEROS 10, Meter Group, Inc.) in a tallgrass prairie at Konza Prairie Biological Station near Manhattan, KS. Collars were maintained vegetation-free throughout the experimental period to assume CO_2 from collars is from heterotrophic soil respiration and B) measuring heterotrophic soil respiration from the installed instrumented PVC collars using a portable infrared CO_2 gas analyzer (model EGM-5, PP Systems, Inc.).

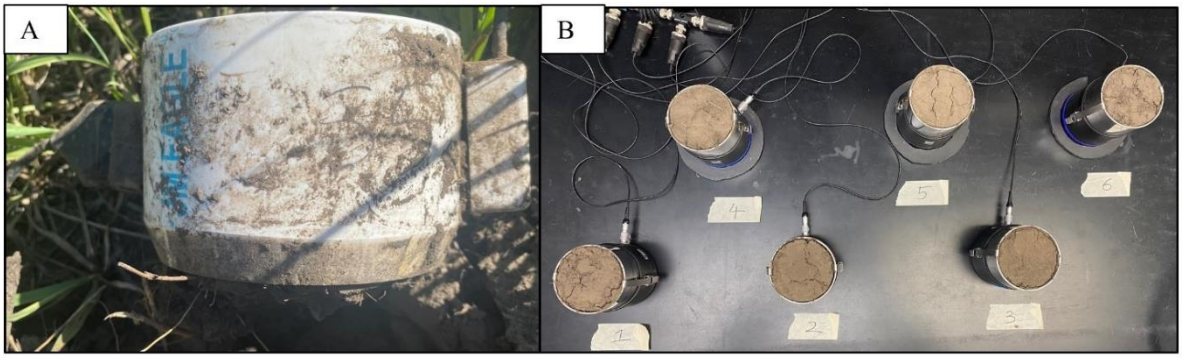

Figure 3-3: A) An excavated instrumented PVC collar at the end of the study period by keeping the soil inside the collar intact. TEROS 21, soil matric potential and temperature sensor at the left side and TEROS 10, soil volumetric water content sensor at the right side of the collar and B) measuring soil matric potential in subsampled soil from excavated instrumented PVC collars under laboratory conditions with Hyprop system (model Hyprop 2, Meter Group, Inc.).

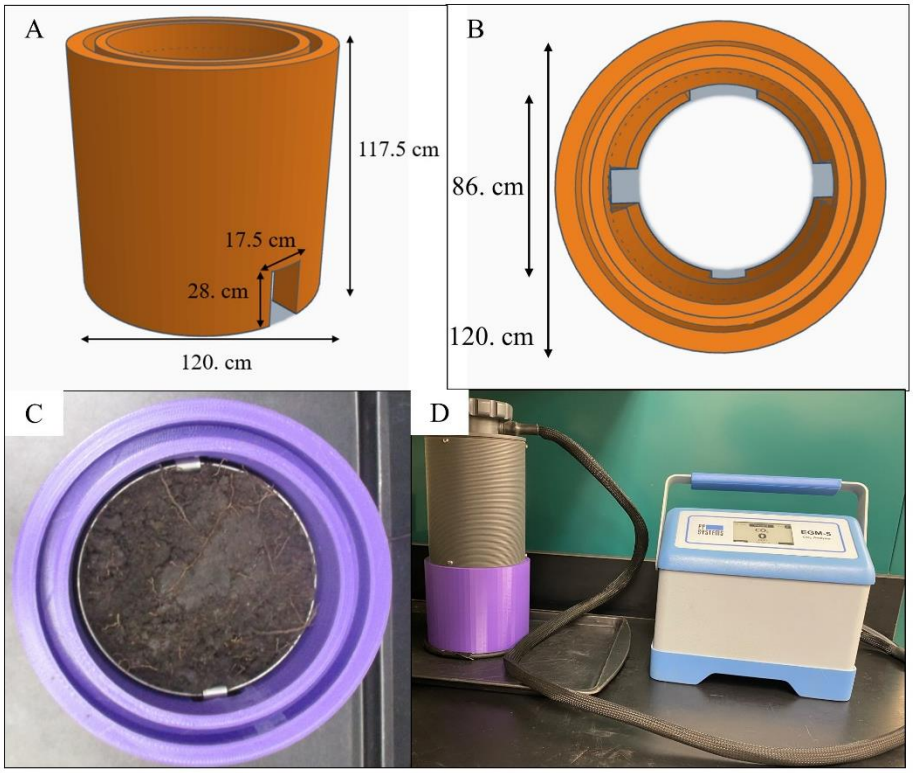

Figure 3-4: A) Side view, B) top view of the designed plastic sleeve for coupling the chamber of portable infrared CO_2 gas analyzer (model EGM-5, PP Systems) with the samples of the Hyprop system (model Hyprop 2, Meter group), C) inserted soil sample mounted on Hyprop system into the 3D printed plastic sleeve for measuring soil CO_2 efflux, and D) simultaneous measurement of soil CO_2 efflux and soil matric potential from a soil sample mounted on Hyprop system.

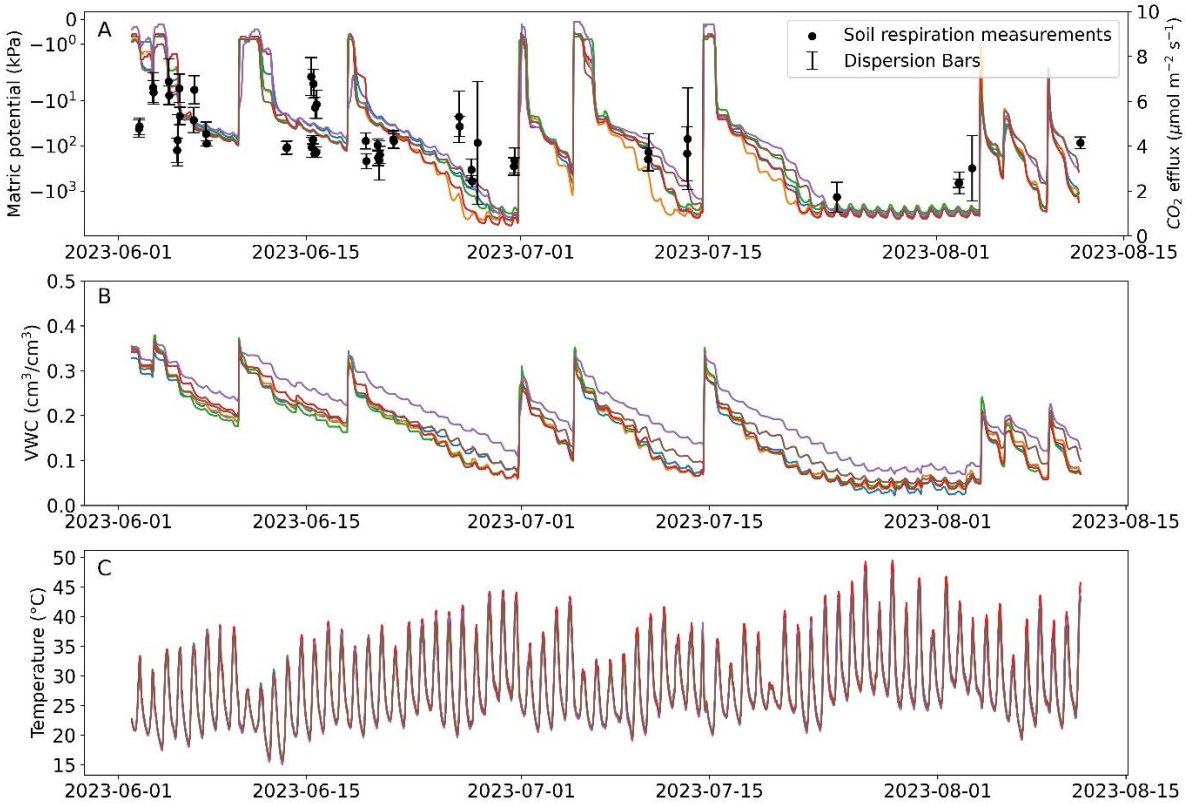

Figure 3-5: A) Soil matric potential, B) volumetric soil water content (VWC), and C) soil temperature at 3.5 cm depth observed from 1 June to 11 August 2023 in a field experiment consisting of six instrumented polyvinyl chloride collars inserted in a tallgrass prairie at the Konza Prairie Biological Station near Manhattan, KS. Soil respiration measurements in Figure 2A represent soil CO_2 efflux values from six instrumented collars for 48 measurements conducted during the experimental period using a portable infrared CO_2 gas analyzer (model EGM5, PP systems, Inc.).

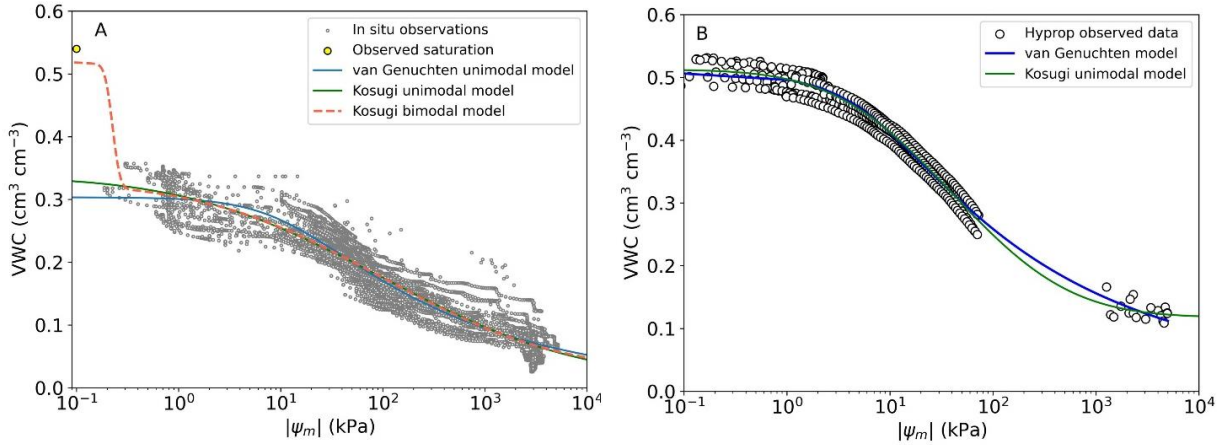

Figure 3-6: A) *In situ* soil water retention curve using hourly observations of soil matric potential (TEROS 21) and volumetric water content (TEROS 10) recorded within the six instrumented collars, B) laboratory-determined soil water retention curves using 250-cm^3 undisturbed subsamples from each of the six instrumented collars using the Hyprop system (model Hyprop 2, Meter group). The unimodal van Genuchten and Kosugi models were fitted to both field and laboratory observations and a bimodal Kosugi model was fitted to the *in situ* observations to account for the effect of soil structure on the pore-size distribution.

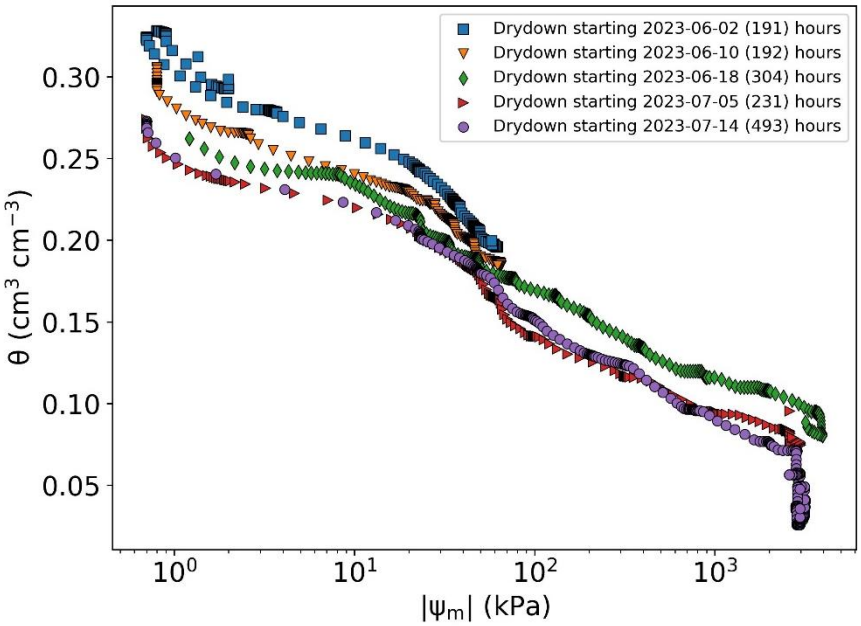

Figure 3-7: Example of *in situ* soil water retention curves using hourly observations of collocated soil matric potential (model TEROS 21, Meter group) and volumetric water content (model TEROS 10, Meter group) for multiple drydown events (i.e., period without measurable precipitation) observed in one of the six collars installed in a tallgrass prairie at the Konza Prairie Biological Station located near Manhattan, KS.

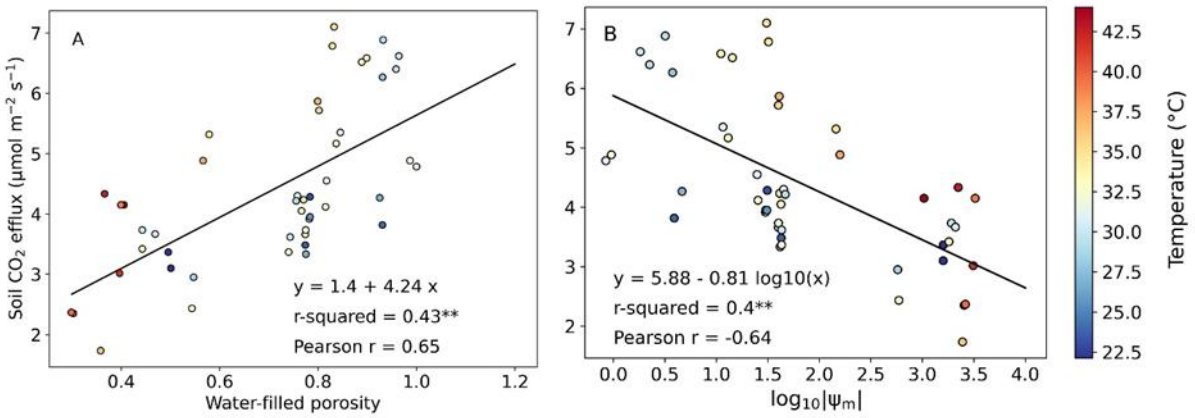

Figure 3-8: Soil CO_2 efflux as a function of A) water-filled porosity and B) soil matric potential with fitted regression line. All field observations were obtained from 1 June to 11 August 2023 using six instrumented collars installed in a tallgrass prairie located within the Konza Prairie Biological Station near Manhattan, KS. Each data point is the average for six collars.

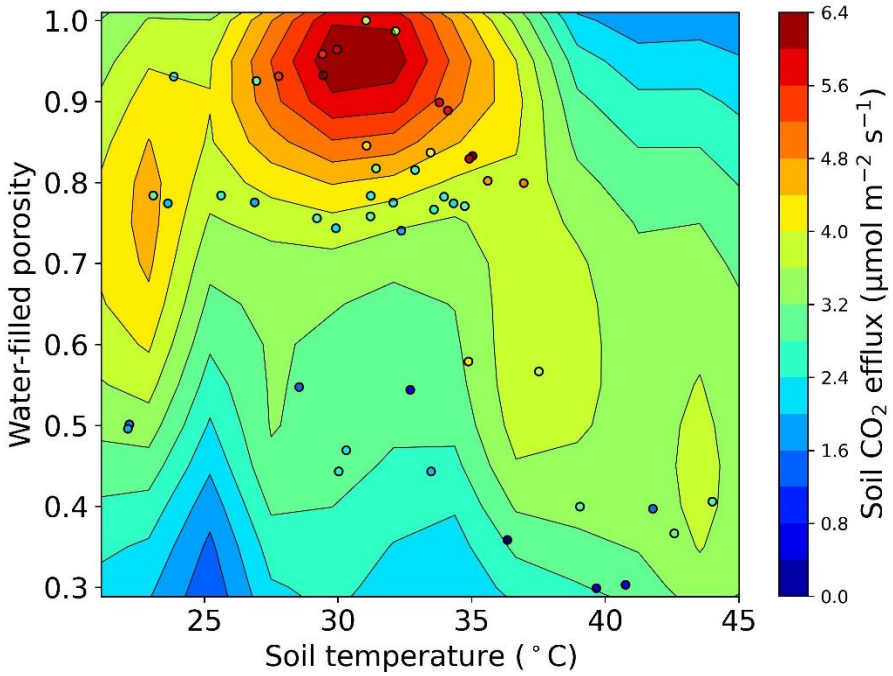

Figure 3-9: Soil CO_2 efflux as a function of soil temperature and water-filled porosity. Each soil CO_2 efflux value is the mean CO_2 efflux from six instrumented collars installed in a tallgrass prairie at Konza Prairie Biological Station, near Manhattan, KS.

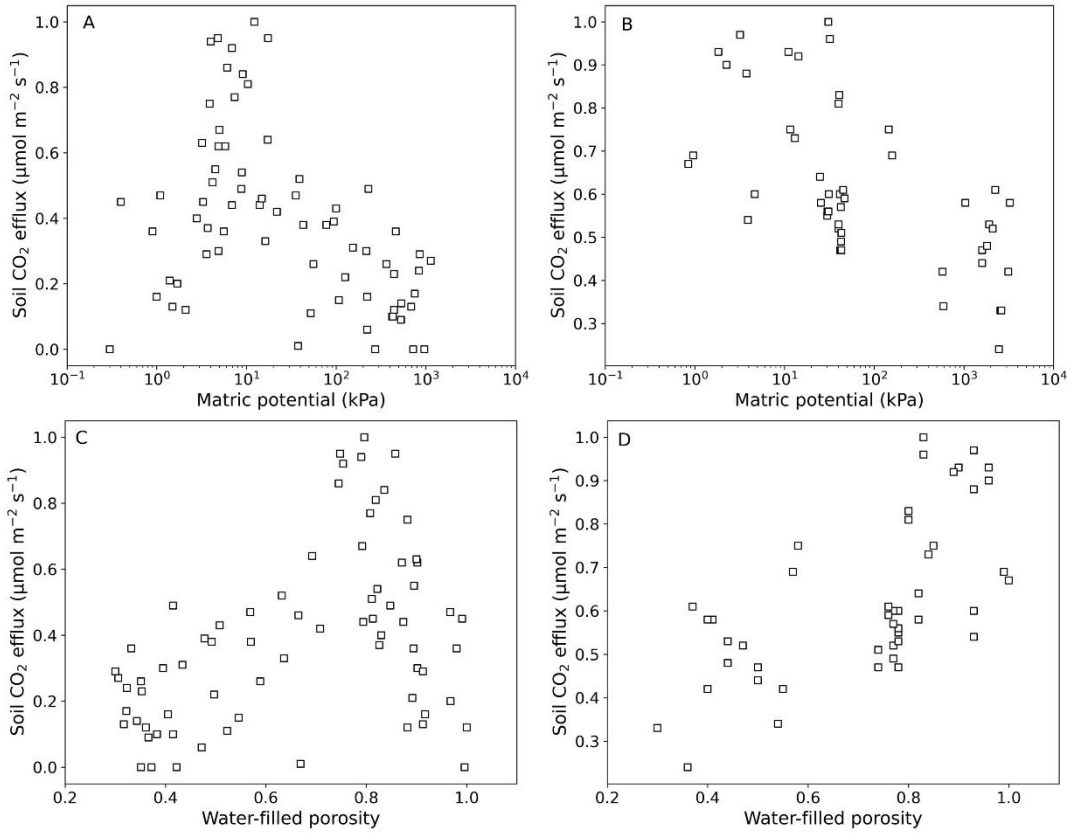

Figure 3-10: Normalized soil CO_2 efflux as a function of soil matric potential A) for sub-sampled soil and B) for *in situ* instrumented collars. Normalized soil CO_2 efflux as a function of water-filled porosity C) for sub-sampled soil and D) for *in situ* instrumented collars. All field observations were obtained using six instrumented collars for measuring soil matric potential, temperature (model TEROS 21, Meter group), volumetric water content (model TEROS 10, Meter group) and soil CO_2 efflux using portable infrared CO_2 gas analyzer (model EGM-5, PP Systems). Collars were installed in a tallgrass prairie located within the Konza Prairie Biological Station near Manhattan, KS. Each data point is the average for six collars. Soil from instrumented collars were sub-sampled at the end of the study and laboratory observations were conducted using sub-sampled undisturbed soil. Soil matric potential under laboratory conditions was measured using mini-precision tensiometers (model Hyprop-2, Meter group) and CO_2 efflux was measured using EGM-5 (PP Systems) CO_2 gas analyzer.

Chapter 4 - General Conclusion

Partitioning soil respiration into its components of autotrophic and heterotrophic respiration is important in understanding ecosystem-level carbon cycling and in identifying the possible different responses of autotrophic and heterotrophic soil respiration to climate change. This thesis aimed at deepening our understanding of the relationship between heterotrophic soil respiration with soil moisture and soil temperature dynamics across different land covers using a series of laboratory and field experiments. The overarching goal of this thesis was to identify unique signatures of the heterotrophic soil respiration during transient soil moisture conditions.

The first chapter focused on understanding the influence of soil water potential and water-filled porosity on heterotrophic soil respiration in laboratory conditions utilizing undisturbed soil samples from three different land covers including cropland, grassland, and riparian areas. The results revealed that land cover type significantly impacts the maximum heterotrophic soil respiration rate, with croplands exhibiting a lower peak heterotrophic respiration rate compared to grasslands and riparian areas. Furthermore, the study highlighted that the simple and easy-to-measure water-filled porosity indicator can be a better predictor of soil respiration compared to soil matric potential. Also, peak heterotrophic soil respiration was consistently achieved at matric potentials similar to that of field capacity (~10 kPa) or at water-filled porosities of ~0.8. The use of the mini-precision tensiometer technique, coupled with simultaneous CO_2 efflux measurements on undisturbed soil samples, provided a better understanding of heterotrophic respiration dynamics across land covers, over traditional methods involving disturbed soil samples.

The second chapter focused on *in situ* measurements of heterotrophic soil respiration with collocated soil matric potential, soil temperature, and volumetric water content. The objective of the study was to investigate the relationship between heterotrophic soil

respiration and soil water potential by coupling *in situ* measurements of soil CO_2 efflux and soil water retention curves (SWRC). Our field experiment revealed bi-modal and time-varying SWRCs that were not observed when the experiment was repeated in laboratory conditions, highlighting the need for more *in situ* measurements, especially to characterize the hydraulic properties in well-aggregated soils. The combination of soil temperature and water-filled porosity allowed us to describe heterotrophic soil respiration which could be used to understand the temporal and spatial dynamics of heterotrophic soil respiration in response to changing soil temperature and moisture conditions. Future studies in this field could combine instrumented collars with automated soil CO_2 chambers to provide deeper insights into the dynamic relationship between soil moisture, soil temperature, and heterotrophic soil respiration, paving the way for more accurate and robust relationships that could be used to improve land surface models.